Legacy effects of precipitation and land use impact maize growth and microbiome assembly under drought stress

Authors

Joel F. Swift[1,2*], Matthew R. Kolp[1,2,4], Amanda Carmichael[1,4], Natalie E. Ford[1], Paige M. Hansen[2,4], Benjamin A. Sikes[1,2], Manuel Kleiner[3], Maggie R. Wagner[1,2*]

Affiliations

[1] Department of Ecology and Evolutionary Biology, University of Kansas, Lawrence, KS 66045

[2] Kansas Biological Survey & Center for Ecological Research, University of Kansas, Lawrence, KS 66045

[3] Department of Plant and Microbial Biology, North Carolina State University, Raleigh, NC, 27695

[4] Current Address: Center for Animal and Human Health in Appalachia, College of Veterinary Medicine, Lincoln Memorial University, Harrogate, TN 37752 (M.R.K.); Department of Conservation and Research, Southeastern Center for Conservation, Atlanta Botanical Garden, Atlanta, GA, 30309 (A.C.); Department of Soil and Crop Science, Colorado State University, Fort Collins, CO 80521 (P.M.H.)

*Correspondence: joel.swift@ku.edu and maggie.r.wagner@ku.edu

Abstract

As the climate changes, plants and their associated microbiomes face greater water limitation and increased frequency of drought. Historical precipitation patterns can leave a legacy effect on soil and root-associated microbiomes, but the impact of this conditioning on future drought performance is poorly understood. Moreover, agricultural practices, like tilling and fertilization, may override precipitation legacies in natural systems. Precipitation gradients provide a means to assess these legacy effects. We collected six soil microbiomes across a Kansas precipitation gradient from both agricultural fields and native prairies. Seedlings of two *Zea mays* genotypes were inoculated with each soil microbiome in a factorial drought experiment. Droughted plants exhibited decreased shoot mass accumulation rates and greater root mass relative to shoot mass.

Restructuring of the bacterial root-associated microbiome was apparent, with depletion observed in Pseudomonadota and enrichment in Actinomycetota, while the fungal microbiome was largely unaffected by drought. A historical precipitation legacy effect on soil microbiomes interacted with plants during drought treatment, but only among prairie soils. Prairie soils from historically wetter locations increased maize shoot biomass under drought more so than agricultural or historically drier prairie soils. We demonstrate links between legacy effects and drought performance, suggesting that future drying climates may condition soils to negatively impact plant performance.

Introduction

Increasing drought frequency due to global climate change will impact both soil and plant-associated microbiomes [1, 2]. Drought directly limits microbial mobility and access to resources, but also alters plant host traits (e.g., root physiology, morphology, and exudate composition) that comprise the habitat available to root-associated microorganisms [3]. Historical precipitation patterns and drought can leave lasting impacts, or legacy effects, on soil and root-associated microbiomes. Naturally-occurring precipitation gradients—which shape the biogeography of both plants [4, 5] and soil microorganisms [6, 7]—provide opportunities to study legacy effects of precipitation on plant-microbe interactions. Historical patterns of water availability across gradients constrain the functional potential of soil microbiomes [8–10]; however, the implications for host plants, including agriculturally critical species, are not well understood.

As plants recruit root microbes primarily from the soil [11], we would expect drought-induced changes in the soil microbiome to be reflected in root-associated microbiomes. However, because many root-associated microbes are also sensitive to plant root traits, their responses to drought may also reflect drought-induced changes in the host phenotype. Both soil- and root-

associated microbiomes under drought exhibit consistent enrichment of gram-positive bacteria and depletion of gram-negative bacteria [12–14]. Within those categories, however, some bacterial phyla respond differently to drought in soil versus roots [3]. For example, enrichment of Bacillota (formerly Firmicutes) and Actinomycetota (formerly Actinobacteria) during drought are less pronounced in soil than in root-associated microbiomes, suggesting that these phyla respond to drought-induced changes in root physiology [14–16]. Thus, drought impacts both soil- and root-associated microbiomes, but in different ways, owing to the influence of the plant phenotype.

Changes in soil- and root-associated microbiomes due to historical precipitation may affect plant fitness under drought. Drought-induced restructuring of root-associated microbiomes is hypothesized to be a conserved mechanism [14, 17] that supports survival of both the plant host and its symbionts [18]. In one study, plant fitness peaked when the soil microbiome's historic moisture conditions matched contemporary experimental conditions [19]. Additional research suggests that exposure to short-term drought creates a microbial legacy effect that moderates drought stress in plants [20, 21] and strengthens positive plant-soil feedbacks, although many such patterns were species-specific [22]. Thus, how historical precipitation patterns condition soil- and root-associated microbiomes and their relevance to plant fitness under drought stress is an open question.

Another open question is how historical sympatry between a plant species and the soil microbiome influences their interactions during drought. For example, drought-stressed *Arabidopsis thaliana* performed better in soil collected from a habitat where the plant had naturalized, compared to soils from a maize field and a forest stand of *Pinus ponderosa* [23]. Conversely, historical sympatry can be detrimental in agricultural systems: soil-dwelling plant pathogens tend to accumulate over time in monocultures [24–26], leading to negative plant-soil

feedbacks [27, 28] that drive lower plant performance in sympatric soils. Agricultural practices such as tillage and irrigation, however, may obscure some of these patterns as has been observed previously [29–31]. Thus, we designed an experiment to assess plant fitness under a contemporary drought when grown in sympatric and non-sympatric conditioned soils from different land use types and historic precipitation regimes.

Our experiment tested how soil microbiomes with different precipitation and land use legacies impacted *Zea mays* L. (maize) under drought stress. We collected six soils across an east-west precipitation gradient in Kansas (Figure 1), representing two land use regimes with differing degrees of sympatry with maize: native prairies and agricultural fields. We inoculated maize seedlings with these soil communities and measured plant growth during our experimental drought. Specifically, we: **1**) characterized plant phenotype and microbiome responses to drought, **2**) tested how soil microbiome histories (precipitation and land use type) affected maize growth, and **3**) identified microbial taxa that were associated with plant growth. A more nuanced understanding of drought-induced phenotypic and root microbiome changes will help stimulate advancements towards alleviating crop losses due to drought.

Material and Methods

Soil inoculum sources and preparation

Soil samples were collected in May 2019 from 4 prairie sites and 2 agricultural sites across a steep precipitation gradient in Kansas, USA (Figure 1). From each site, ~60 cm deep samples were collected from each corner and the center. The first 2-3 cm of topsoil were removed. Soil samples were homogenized, sieved, and stored in plastic bags at 4ºC until use (~4 months after collection).

Inocula were prepared by mixing 20 g of each soil into 100 mL 1x phosphate-buffered saline (PBS) and 0.0001% Triton X-100. After settling, the mixtures were filtered through Miracloth (22-25 µm pore size; Calbiochem, San Diego, CA, USA) and then centrifuged for 30 minutes (3000 x g). After discarding the supernatant, the microbial pellets were resuspended in 20 mL 1x PBS; these slurries were kept shaking for aeration until use, later that day. Each final inoculum consisted of 10 mL soil slurry in 1 L 0.5X Murashige and Skoog basal salt mixture (MS; Sigma-Aldrich, Darmstadt, Germany). A control treatment was made by adding 10 mL sterile 1x PBS into 1 L 0.5X MS.

Planting, inoculation, and greenhouse setup

To increase the generalizability of our results, two genotypes of *Zea mays* L. (maize) were used: B73 and Mo17 [32]. In a laminar flow hood, seeds were surface sterilized by submerging in 70% ethanol, then 5% NaClO, followed by three rinses with sterile water. To avoid confounding effects of soil physicochemical properties, autoclaved calcined clay ("Pro's Choice Rapid Dry"; Oil-Dri Corporation, Chicago, IL) was used as the growth medium. Seeds were planted one inch deep in 107 mL "Cone-tainers" (Stuewe & Sons Inc., Tangent, OR, USA). Cone-tainers were assigned randomly to treatments, inoculated with 25 mL of one of the six soil inocula (or the sterile control), and placed two inches apart in randomized complete blocks (Figure S1A) containing the 24 treatment combinations and one of four controls. Plants were arranged under growth lights (250 W Sun Systems Compact Cool fluorescent lamps) to supplement natural light for 13 hours/day during the experiment (January-March 2020).

Monitoring and harvesting plants

All plants received 30 mL of reverse osmosis water twice weekly until emergence. After emergence, "well-watered" plants continued twice-weekly watering while "droughted" plants

were watered every 8-12 days. Plant height was measured weekly to the nearest 0.25 cm on the tallest fully expanded leaf held parallel to the stem. Plants were sequentially harvested to measure biomass at one of three time points during the experiment: 100 plants on day 24 and day 39, and the remainder (n=344) on day 50 (Figure S1B). Calcined clay was removed from roots by hand. Shoot and root fractions were separated and oven-dried at 65 ºC to a constant weight. Before drying, one nodal root (from the uppermost soil-borne root whorl) per plant was collected and stored at -80 ºC until DNA extraction.

Phenotypic analysis

All statistical analysis for phenotypic and microbiome data (see below) was conducted in R v3.6 [33]. Differences among group means were assessed using analysis of variance (ANOVA) with Type III sums of squares in the car v3.0.13 [34] or lmertest v3.1.3 packages [35] with post-hoc comparisons made using the emmeans package v1.7.4.1 [36]. Assumptions of all models were checked by inspecting model residuals [37]. Dry shoot and root mass were converted to accumulation rates (g/day) to account for the variable number of growing days plants experienced post-emergence. The lme4 package v1.1.29 [38] was used to fit a generalized linear mixed model for emergence (binary) and linear mixed models for other growth responses (continuous). Models used the following formula (*growth response~ Inoculum* × *Treatment* × *Genotype*) with all possible interactions included. Models were also fit using '*Longitude*' instead of '*Inoculum*' to test the linear relationship between plant growth and the longitude of the soil microbiome origin sites (a proxy for mean annual precipitation; Figure 1). Experimental block was treated as a random effect with time point included as an additional random effect in the root/shoot ratio model. Root/shoot ratio was log-transformed and both shoot and root mass rate were square-root-transformed to meet the assumptions of ANOVA.

DNA extraction and library preparation

Nodal roots were freeze-dried for 48 hours (FreeZone lyophilizer; Labconco, Kansas City, MO, USA) and ground to powder with a HT Lysing Homogenizer (OHAUS, Parsippany, NJ, USA). Each ground root sample was mixed into 800 µL lysis buffer (1M Tris pH=8.0; 0.5 mM NaCl; 10 mM EDTA) and transferred to 96-well plates containing 500 µL 1 mm garnet rocks per well (Biospec Products, Bartlesville, OK, USA), after which DNA purification proceeded via bead-beating and chemical lysis as previously described [39]. DNA from soil and freshly generated inocula samples was extracted in December 2022 using the same protocol but omitting the lyophilization step and placing 250 mg soil or 800 µL inoculum directly into a garnet plate.

Amplicon sequencing libraries were prepared using established protocols [39]. Briefly, we PCR-amplified the V4 region of the 16S rRNA gene and ITS1 region for bacteria and fungi, respectively. Amplicons were sequenced (2x250 bp) on a NovaSeq 6000 SP flow cell (Illumina, San Diego, CA, USA). Each "batch" of 96 samples remained together throughout DNA extraction, amplification, and sequencing.

Bioinformatic processing

Sequence processing and quality filtering was conducted using an established workflow [39]. Briefly, Cutadapt v2.3 [40] was used to remove primers and demultiplex sequences into 16S and ITS sequence files. DADA2 v1.14.1 [41] was used to denoise reads, merge paired-end sequences, dereplicate, and remove chimeric sequences. Taxonomy was assigned to the resulting amplicon sequence variants (ASVs) by a naïve Bayesian classifier [42] trained on the 11.5 release of the Ribosomal Database Project [43] for bacteria and the 01.12.2017 release of the UNITE database [44] for fungi. Phyloseq v1.40.0 [45] was used to remove host contamination and ASVs unassigned to a kingdom. Chao1 richness and diversity indices (Shannon and Inverse Simpson)

were calculated before the removal of ASVs not observed ≥25 times in ≥5 samples and samples with <400 reads. Finally, ASV counts were centered-log-ratio (CLR) transformed using the ALDEx2 package v1.28.1 [46, 47].

Microbiome Analysis

To test the similarity of inocula to their soils of origin, a linear model was fit for each alpha diversity metric with collection site, substrate (soil *vs.* inoculum), and sequencing depth (Z-transformed) as main effects. Community composition was assessed by permutational multivariate analysis of variance (PERMANOVA) and constrained partial redundancy analysis (RDA). For PERMANOVA, the *adonis2()* function from the vegan package v2.6.2 [48] was used to model the matrix of between-sample Aitchison distances [47] with collection site and substrate as main effects. The RDA was fit with the same model, removing variance attributed to log(Sequencing Depth), and visualized using an ordination plot.

To investigate root microbiome responses, a model was fit for each alpha diversity metric (*Metric ~ Soil Inoculum × Drought Treatment + Genotype*), with *Block* and *Batch* as random effects. Genotype was treated as a fixed effect without interactions to generalize results across genotypes and increase power to detect other main effects. Each phylum's CLR-transformed abundance was modeled to test for responses to experimental factors. Across all models and where appropriate, p-values were adjusted to correct for multiple comparisons using a Benjamini-Hochberg correction [49]. To explore changes in community composition, a PERMANOVA model was fit (*Aitchison matrix ~ Soil Inoculum × Drought Treatment + Genotype*) with permutations constrained by *Batch.* Main effects were tested for homogeneity of dispersions using the vegan package. Pairwise dispersions among factor levels were assessed using a permutation test with 999 permutations constrained by *Batch.* Constrained partial redundancy analysis of the

Aitchison distance matrix was conducted to remove variance attributed to *Batch* and *log(Sequencing Depth)* and to visualize the variance in microbial composition explained by experimental factors.

The machine-learning package caret v6.0.92 [50] with ranger's v0.14.1 [51] implementation of the random forest algorithm was used to assess how accurately roots could be classified as droughted or well-watered based on microbiome community data (bacterial and fungal, separately). Samples were randomly split into a training set (80%) and a test set (20%), with the test set withheld from the model, and used to determine the final model's performance. Hyperparameters were optimized using a grid search over minimum node size (1, 5, 10) and the number of features available at each node (10-100% of the ASVs). For each combination in the grid, classifier accuracy was used to assess performance on out-of-bag samples with 10-fold cross validation. Final predictions were made with the trained model on the withheld test set and visualized using confusion matrices. The contribution of each ASV to classification accuracy was assessed using permuted importance: mean decrease in accuracy (MDA) values were calculated for each ASV across the 10-fold cross validation. The benefits of this strategy are twofold, we can assess if drought induced a predictable shift in the microbiome as a whole and identify individual ASVs with the greatest differential abundance as a result of drought.

Connecting plant growth responses to microbial abundances

Linear models were used to test associations between taxon abundances and plant growth. To focus on the phenotypic variation that could not be explained by Genotype, Inoculum, Block and Batch effects, we extracted residuals from a model that contained these terms and used them as the response variable for a second model ($Growth\ Response_{residual} \sim Taxon\ abundance \times Drought\ Treatment$). *Taxon abundance* described the association of the taxon (CLR-transformed

counts of bacterial families and fungal orders) with plant growth rate; the interaction term described whether the taxon's effect on plant growth differed under droughted vs. well-watered conditions.

Results

Soil and inocula community composition differs across collection sites

We assessed the microbial community composition of soils and their derived inocula from the six collection sites (n = 8 per site). Bacterial and fungal alpha diversity of soils differed across collection sites (Tables S2 and S3); bacterial diversity was highest in the westernmost prairie soil whereas fungal diversity was highest in the easternmost prairie soil (Figures S2 and S3). Additionally, community composition of both bacterial and fungal microbiomes differed among sites (Table S3; R^2=0.22-0.23; *p*-value<0.01). Relative abundances of bacterial phyla and fungal classes further showed site-specific patterns (Figures S4 and S5), however, few were correlated with longitude.

Relative to the original soils, the inocula had similar bacterial alpha diversity but lower fungal richness (Figure S3C-D; Tables S2 and S3). The composition of both bacterial and fungal communities also shifted between soils and their derived inocula (Table S4); however, both soil and inocula samples clustered in ordination space by collection site (Figure 2). Thus, the original soil microbial communities were largely retained in the derived inocula.

Plant responses to soil microbiomes vary across genotype and drought treatment

We found no evidence that soil inocula impacted emergence rates (*p*-value = 0.37, Pearson's χ^2 test; Table S1), however, maize genotype B73 (82.5%) emerged more successfully than Mo17 (62.0%; *p*-value=0.05, Pearson's χ^2 test). Post-emergence, both drought treatment and

maize genotype affected plant growth responses (Table 1). Drought decreased both shoot and root mass accumulation rates (Figure 3A-B; *p*-value=<0.01) and increased root/shoot ratio (Figure 3C; *p*-value<0.01). These traits also differed between genotypes, with Mo17 investing more into root growth than B73 (Figure S6; *p*-value=<0.01). Shoot mass rate was the only trait that responded to soil inoculum (Table 1; *p*-value=<0.01); this effect was driven by the 'TLI$_P$' inoculum, which slowed the accumulation of root mass.

We observed no evidence of interactions between drought treatment and soil inoculum on plant growth responses. However, inoculum interacted with genotype to influence root/shoot ratio (Table 1; *p*-value=0.02). Mo17 displayed greater root/shoot ratios than B73 across all inocula, although the magnitude of this difference varied (Δ_{emmean} 0.176-0.493; *p*-value=0.02-<0.01). B73 accumulated shoot mass more quickly than Mo17 when inoculated with three of the four prairie soil microbiomes ('SVR$_P$' *p*-value=<0.01, 'HAY$_P$' *p*-value=<0.01, 'TLI$_P$' *p*-value=0.03, 'KNZ$_P$' *p*-value=0.27) but not with agricultural soil microbiomes ('SVR$_{Ag}$' *p*-value=0.33, 'TLI$_{Ag}$' *p*-value=0.12). Thus, the effect of soil microbial communities on maize growth generally depended on plant genotype, but not on the drought treatment.

Root microbiomes and community responses to drought modulated by soil inoculum

Drought treatment and soil inocula collection site impacted the richness and diversity of root-associated bacterial and fungal communities (Tables S5 and S6). Drought increased Chao1 richness of bacterial communities (Tables S5 and S6; *p*-value=0.01) but affected neither Shannon nor Inverse Simpson diversity. In contrast, Shannon and Inverse Simpson fungal diversity increased under drought conditions, particularly for plants that received the 'TLI$_P$' inoculum (Figure 1A; Table S6; *p*-value=0.01–0.02).

Bacterial community composition depended on the soil inoculum (Table 2; R^2=0.05, *p*-value=<0.01, PERMANOVA) and drought treatment (R^2=0.01, *p*-value=<0.01, PERMANOVA). We found no evidence that bacterial community dispersion differed among treatments, genotypes, or inocula (*p*-value=>0.05, Multivariate Levene's test). Redundancy analysis aligned with PERMANOVA results: soil inoculum and drought treatment explained the largest proportions of variance (6.09% and 1.57%; Figure S7 and 4B, respectively), while genotype explained >1% of variance (Figure S8). We attributed 7.1% of the variance in Deinococcota (formerly Deinococcus-Thermus) to the interaction between soil inoculum and drought (*q*=0.03), with enrichment observed in droughted plants (39.6% increase in relative abundance). In addition, 3.7% of the variance in Pseudomonadota was attributable to our drought treatment (*q*=0.04); relative abundance of this phylum decreased 4% in droughted plants.

In contrast, drought treatment did not alter relative abundances of any fungal classes, nor overall root fungal community profiles (Figure 5A). Variance in fungal community composition was mostly due to initial soil inoculum source (Figure S9; Table 3; R^2=0.09, *p*-value=<0.01). As observed for bacterial communities, neither drought treatment, maize genotype, nor soil inoculum source affected fungal community dispersion (*p*-value=>0.05, Multivariate Levene's test). Drought and maize genotype each explained <1% of the variance in fungal community composition (Figure 5B and S10, respectively). Thus, while root-associated bacterial community composition responded weakly to drought treatment, we observed no trend for fungal community composition.

Identification of bacterial and fungal ASVs responding to drought

Our random forest models showed greater accuracy in predicting the drought treatment of a given sample when trained on bacterial vs fungal communities (Figure 4C&5C). Two bacterial

ASVs from the genus *Sphingomonas* (Pseudomonadota) were the top two features contributing to prediction accuracy of the random forest classifier when attempting to predict drought treatment, with a mean decrease in accuracy (MDA) of 2.88% and 0.59% when withheld from the model (Figure 4C and S11-12). In other words, these two bacterial ASVs contributed to ~3.5% increase of model accuracy in predicting drought and were positively correlated with one another (*p*-value=<0.01; r=0.521 Pearson test). These *Sphingomonas* ASVs were depleted in droughted plants relative to well-watered plants (10.8% decrease in relative abundance). In contrast, we did not detect any fungal ASVs that were differentially abundant in response to drought treatment, nor any that contributed to random forest classifier accuracy with MDA value >0.5% (Figure 5C and S13-14).

Connecting plant growth responses to bacterial and fungal communities

Soil inocula derived from collection sites across Kansas, spanning an east-west precipitation gradient had only a small impact on plant growth responses (Table 1; Figure 6A and S15). These patterns were not correlated with the longitude of soil inocula collection sites (a proxy for precipitation) when including both agricultural sites and native prairies (Figure S16; *p*-value=0.08-0.70 and 0.17-0.93; ANOVA for *'Longitude'* and *'Longitude × Treatment'*, respectively). However, when restricting the analysis to prairie soil communities, we detected an interaction between longitude and drought treatment (Figure 6B; *p*-value=0.03). The shoot mass rate of well-watered plants was negatively associated with longitude (slope=-3.29e^{-4} g/day/°longitude) whereas droughted plants displayed a weak positive association (slope=3.04e^{-5}). Put another way, plants that experienced drought benefited from microbiomes from historically wetter soils, while the opposite was true for well-watered plants in the experiment. Notably, B73

and Mo17 exhibited contrasting associations with longitude and soils across the Kansas precipitation gradient (Figure 6C; *p*-value=0.03; Slope=-3.07e^{-4} and 9.12e^{-6}, respectively).

We identified bacterial and fungal taxa correlated with promotion or repression of plant growth. Overall, 13 bacterial families showed a significant positive (6/13) or negative (7/13) growth promotion effect on shoot mass (Table 4). These represented only a few phyla (6 Actinomycetota, 5 Pseudomonadota, and 2 Bacillota) and were predominantly gram positive (8/13). Two of the identified families (Corynebacteriaceae and Streptococcaceae) interacted with drought treatment, indicating that their effect on shoot mass rate was modulated by the amount of water the plant received. The abundances of Corynebacteriaceae and Streptococcaceae were negatively correlated with shoot mass rate in well-watered plants but not in droughted plants (Figure S17). Using the same analysis framework, root mass rate was not associated with any bacterial families, possibly because root mass rate variance decreased over time as plant roots expanded to fill the entire container (Figure S18). In addition, bacterial families that correlated with root/shoot ratio were simply a subset of the bacterial families identified for shoot mass rate. For fungi, only shoot mass rate showed significant correlations with the abundance of fungal orders (Table 5). All three significant fungal orders (Hypocreales, Malasseziales, and Sporidiobolales) were positively correlated with shoot growth regardless of the water regime applied.

Discussion

Understanding plant-microbiome interactions under drought stress is critical to safeguard agricultural systems in the face of global climate change. In this study, we measured the growth of maize seedlings under experimental drought after inoculation with soil microbiomes from across a natural precipitation gradient in Kansas. Under drought stress, we observed phenotypic

differences in maize resource allocation and the restructuring of bacterial, but not fungal, root microbiome communities. Following the stress gradient hypothesis [52] we expected drought-stressed maize seedlings to perform better in the presence of microorganisms from historically dry soils, where chronic water stress would have fostered positive interactions with neighboring plants. We detected an effect of historical precipitation exposure on soil microbiomes' interactions with plant hosts during drought treatment, but only for the prairie soils. Notably, the direction of this interaction was opposite of our prediction: prairie soils from historically wetter locations increased maize biomass under experimental drought more than soils from historically dry locations. Deeper analysis revealed several bacterial and fungal taxa that were associated with plant growth promotion or repression and that were modulated by the experimental drought.

Plant and microbiome responses to drought

In our experiment, maize displayed strong phenotypic tradeoffs in response to drought. Drought-treated plants increased root growth relative to shoot growth, resulting in shorter plants over the course of the experiment. This supports our understanding of plant responses to drought, as plants prioritize root over shoot growth under drought stress [53, 54], favoring deeper and often denser root systems in order to obtain sufficient water [55–57]. These phenotypic changes in root growth, along with direct effects of water limitation in the soil, contributed to the responses of the root microbiomes in our study.

Drought altered bacterial communities of maize roots, although the magnitude of compositional change within our study was small (R^2=0.01) relative to other studies (R^2=0.04-0.10) [14–16, 18]. Similar to previous studies [17], we observed a depletion of gram-negative and an enrichment for gram-positive bacteria in response to drought, likely relating to the desiccation resistance provided by the single thick peptidoglycan cell wall of gram-positive bacteria [58].

Enrichment of Actinomycetota during drought tends to be more pronounced in root-associated microbiomes than in soil, suggesting that shifts in plant root physiology also play a role [3, 17]; however, the root traits driving this effect are unknown. During drought, root exudate quantity is generally maintained or increased [59–61], but the stronger changes in exudate composition [62–64] may contribute to the root microbiome drought response [65]. In *Sorghum*, for instance, drought-induced changes in root exudate composition and iron homeostasis contribute to Actinomycetota enrichment in the rhizosphere [18, 66].

Fungal communities of maize roots were less sensitive to drought relative to their bacterial neighbors. While drought increased the diversity of the plants inoculated with the TLI prairie fungal community, it did not significantly affect overall fungal community composition. Machine learning classification by drought treatment further illustrated this difference: when trained on bacteria, we achieved 72.5% balanced accuracy, while for fungi, we achieved only 50%. This cross-kingdom difference agrees with previous reports, as both free living and root-associated fungal communities tend to tolerate desiccation [67, 68]. The observed difference in survival between bacteria and fungi under drought may relate to both the vegetative and dormant growth forms of fungi: hyphae comprise most vegetative fungal growth and can cross air-gaps within dry soil in search of resources [58, 69], and dormant spores are generally desiccation-resistant [70].

Historical precipitation, soil community legacies, and their impact on plant drought tolerance

Our hypothesis that historical precipitation patterns would impart legacy effects on soil microbiomes that influence plant growth under drought stress was partially supported. Bacterial and fungal compositional differences were apparent among the soils and inocula from six sites across a steep precipitation gradient in Kansas (Figure 1&2). In the four soils from prairie sites, we found a significant interaction for shoot mass rate between longitude of soil inoculum source

and drought treatment. The fact that the two agricultural soils weakened this pattern provides support for our hypothesis: the periodic irrigation of the agricultural sites may have obscured the legacy effects of historic differences in annual rainfall across the gradient. Alternatively (or in addition), intensive agricultural practices such as tillage and fertilization may have altered these soil microbiomes in a way that disrupted their responses to drought and/or their interactions with the host plant.

Interestingly, we found plants performed better when the historic conditions were opposite the contemporary conditions. The reason for this surprising result is not immediately clear, but there are several possible explanations. Contemporary well-watered conditions may have relaxed the fitness consequences of expression of microbial traits that are critical under drier environments. For instance, microorganisms counteract the physiologic stress of drought by accumulating solutes, which reduces their internal water potential as a mechanism to avoid desiccation [71]. The accumulation of solutes requires considerable energy expenditure and constitutes a large sink of C and N resources [72–74]. The contemporary well-watered conditions relax these costly solute needs, perhaps allowing resources to be reallocated to functions that are beneficial to plants. Another possibility is that soils from historically wetter sites generally possess greater microbial biomass and diversity [75–77], which is predicted to promote positive interactions and improved community function [78]. A third potential explanation involves the balance of beneficial and pathogenic microbes in the soil community. Pathogen richness in soil, root, and shoot microbiomes is often positively associated with mean annual temperature and precipitation [79–81]. Thus, soil communities from historically dry sites may have relatively fewer plant pathogens, resulting in greater plant performance under contemporary well-watered conditions. We cannot distinguish between these possible explanations using the data in hand; however, a future experiment that

leverages rain exclusion structures could effectively explore changes in the balance of beneficial, neutral, and pathogenic microbes.

The degree of sympatry between the plant species and the soil microbiome may affect performance under drought conditions for the host plant [20, 23]. Positive plant-soil feedbacks are generally expected to strengthen under drought conditions [82, 83], but this effect can vary strongly by plant species and functional group [84, 85]. Irrigation of agricultural sites would have weakened historical drought stress, and in turn reduced positive interactions [52]. Furthermore, repeated growth of a crop in one location, even in rotation with another species, frequently results in negative feedbacks driven by soil microbial communities [86–88]. Therefore, we expected that maize inoculated with agricultural soil microbiomes (*i.e.,* from grain fields where maize has long been a dominant plant species) would perform worse under drought than plants inoculated with prairie soils that were naïve to maize. Consistent with our expectation, inoculation with prairie-derived communities increased shoot mass rate and root/shoot ratio in the maize genotype B73, relative to farm-derived communities. This finding agrees with past work showing that frequent cultivation of maize in monoculture can lead to a buildup of pathogenic microbes in the soil and stronger negative plant-soil feedbacks [24–26, 89]. The prairie soils, naïve to maize, would have had no such buildup. Our results support the need for additional research to tease apart the ability of dominant plant species to condition soil microbiomes in either a beneficial or detrimental manner, and to characterize the environmental dependency of such conditioning.

Microbial taxa associated with plant growth

Although only a small portion of plant growth variance was explained by soil inoculum source and historical precipitation, we identified multiple bacterial and fungal taxa that correlated with plant growth responses to drought. Two bacterial families, Corynebacteriaceae and

Streptococcaceae, repressed growth of well-watered but not droughted plants. Corynebacteriaceae has been recovered from roots of multiple plant species [90, 91] and been identified as a keystone species of the endosphere in two Antarctic endemic plants [92]. This family contains multiple phytopathogenic species [93] with some strains specific to maize [94]. Additionally, during a multi-generation experimental evolution study, Corynebacteriaceae (among other bacterial families) was consistently associated with delayed flowering in multiple plant species [95]. Less is known about the relevance of Streptococcaceae to plant growth. In *Zingiber officinale*, this family was significantly enriched in rhizomes with advanced stages of soft rot [96]. However, Streptococcaceae is prevalent in soil and plants [97, 98], typically at higher abundance in aerial plant compartments than in the rhizosphere [99, 100]. Both of these families represent targets for direct manipulation and *in-planta* testing to better understand the mechanism responsible for the growth repression we observed under well-watered conditions.

Acknowledgements

We thank members of the Wagner lab for helpful comments in preparing this article. In addition, we thank Zachary Harris and Nichole Ginnan for helpful discussions. This work was funded by the United States Department of Agriculture National Institute of Food and Agriculture (USDA-NIFA) grant #2022-67013-36672 to MK and MRW, National Science Foundation grant #IOS-2016351 to MRW, Novo Nordisk Foundation INTERACT project under award number NNF19SA0059360 to MK, and seed funding from the NSF under award No. OIA-1656006 to Dr. Kristin Bowman-James and matching support from the State of Kansas through the Kansas Board of Regents.

Competing Interests

The authors declare that the research was conducted in the absence of any commercial or financial relationships that could be construed as a potential conflict of interest. Any opinion, findings, and conclusions or recommendations expressed in this material are those of the authors and do not necessarily reflect the views of the United States Department of Agriculture or the National Science Foundation.

Data Availability Statement

Raw sequencing data is available on NCBI SRA under BioProject ID PRJNA913622 and SRA accessions SAMN32302538-SAMN32303072 for root-associated samples and SAMN33863891-SAMN33864082 for soil and inoculum samples. Code to reproduce the analysis and figures are available on GitHub at https://github.com/Kenizzer/Maize_Drought_Microbiome.

Author Contributions

BAS and PMH collected soil samples across Kansas. MRK, MK, and MRW designed the experiment and collection methods. MRK performed sample collection and processing. AC and NEF performed DNA extractions and library preparations. NEF and JFS performed the data analysis. JFS wrote the first draft of the manuscript. All authors contributed to data interpretation, the writing and reviewing of the manuscript, and approved the final draft.

References

1. Balting DF, AghaKouchak A, Lohmann G, Ionita M. Northern Hemisphere drought risk in a warming climate. *npj Clim Atmos Sci* 2021; **4**: 61.

2. Chiang F, Mazdiyasni O, AghaKouchak A. Evidence of anthropogenic impacts on global drought frequency, duration, and intensity. *Nat Commun* 2021; **12**: 2754.

3. Naylor D, Coleman-Derr D. Drought Stress and Root-Associated Bacterial Communities. *Front Plant Sci* 2018; **8**: 1–16.

4. Korell L, Auge H, Chase JM, Harpole WS, Knight TM. Responses of plant diversity to precipitation change are strongest at local spatial scales and in drylands. *Nat Commun* 2021; **12**: 2489.

5. Field R, Hawkins BA, Cornell H V., Currie DJ, Diniz-Filho JAF, Guégan J-F, et al. Spatial species-richness gradients across scales: a meta-analysis. *J Biogeogr* 2009; **36**: 132–147.

6. Bachar A, Al-Ashhab A, Soares MIM, Sklarz MY, Angel R, Ungar ED, et al. Soil Microbial Abundance and Diversity Along a Low Precipitation Gradient. *Microb Ecol* 2010; **60**: 453–461.

7. Hawkes C V., Kivlin SN, Rocca JD, Huguet V, Thomsen MA, Suttle KB. Fungal community responses to precipitation. *Glob Chang Biol* 2011; **17**: 1637–1645.

8. Hawkes C V., Keitt TH. Resilience vs. historical contingency in microbial responses to environmental change. *Ecol Lett* 2015; **18**: 612–625.

9. Averill C, Waring BG, Hawkes C V. Historical precipitation predictably alters the shape and magnitude of microbial functional response to soil moisture. *Glob Chang Biol* 2016; **22**: 1957–1964.

10. Canarini A, Schmidt H, Fuchslueger L, Martin V, Herbold CW, Zezula D, et al. Ecological memory of recurrent drought modifies soil processes via changes in soil microbial community. *Nat Commun* 2021; **12**: 5308.

11. Zarraonaindia I, Owens SM, Weisenhorn P, West K, Hampton-Marcell J, Lax S, et al. The Soil Microbiome Influences Grapevine-Associated Microbiota. *MBio* 2015; **6**: e02527-14.

12. Acosta-Martínez V, Cotton J, Gardner T, Moore-Kucera J, Zak J, Wester D, et al. Predominant bacterial and fungal assemblages in agricultural soils during a record drought/heat wave and linkages to enzyme activities of biogeochemical cycling. *Appl Soil Ecol* 2014; **84**: 69–82.

13. Fuchslueger L, Bahn M, Hasibeder R, Kienzl S, Fritz K, Schmitt M, et al. Drought history affects grassland plant and microbial carbon turnover during and after a subsequent drought event. *J Ecol* 2016; **104**: 1453–1465.

14. Naylor D, DeGraaf S, Purdom E, Coleman-Derr D. Drought and host selection influence bacterial community dynamics in the grass root microbiome. *ISME J* 2017; **11**: 2691–2704.

15. Santos-Medellín C, Edwards J, Liechty Z, Nguyen B, Sundaresan V. Drought Stress Results in a Compartment-Specific Restructuring of the Rice Root-Associated Microbiomes. *MBio* 2017; **8**: 1–15.

16. Fitzpatrick CR, Copeland J, Wang PW, Guttman DS, Kotanen PM, Johnson MTJ. Assembly and ecological function of the root microbiome across angiosperm plant species. *Proc Natl Acad Sci* 2018; **115**: E1157–E1165.

17. Xu L, Coleman-Derr D. Causes and consequences of a conserved bacterial root microbiome response to drought stress. *Curr Opin Microbiol* 2019; **49**: 1–6.

18. Xu L, Naylor D, Dong Z, Simmons T, Pierroz G, Hixson KK, et al. Drought delays development of the sorghum root microbiome and enriches for monoderm bacteria. *Proc Natl Acad Sci* 2018; **115**: E4284–E4293.

19. Lau JA, Lennon JT. Rapid responses of soil microorganisms improve plant fitness in novel environments. *Proc Natl Acad Sci* 2012; **109**: 14058–14062.

20. Kaisermann A, de Vries FT, Griffiths RI, Bardgett RD. Legacy effects of drought on plant–soil feedbacks and plant–plant interactions. *New Phytol* 2017; **215**: 1413–1424.

21. De Long JR, Semchenko M, Pritchard WJ, Cordero I, Fry EL, Jackson BG, et al. Drought soil legacy overrides maternal effects on plant growth. *Funct Ecol* 2019; **33**: 1400–1410.

22. Buchenau N, van Kleunen M, Wilschut RA. Direct and legacy-mediated drought effects on plant performance are species-specific and depend on soil community composition. *Oikos* 2022; **2022**: 1–14.

23. Zolla G, Badri D V., Bakker MG, Manter DK, Vivanco JM. Soil microbiomes vary in their ability to confer drought tolerance to Arabidopsis. *Appl Soil Ecol* 2013; **68**: 1–9.

24. Strom N, Hu W, Haarith D, Chen S, Bushley K. Interactions between soil properties, fungal communities, the soybean cyst nematode, and crop yield under continuous corn and soybean monoculture. *Appl Soil Ecol* 2020; **147**: 103388.

25. Sumner DR, Gascho GJ, Johnson AW, Hook JE, Threadgill ED. Root Diseases, Populations of Soil Fungi, and Yield Decline in Continuous Double-Crop Corn. *Plant Dis* 1990; **74**: 704.

26. Wachowska U, Rychcik B. Plants control the structure of mycorrhizal and pathogenic fungal communities in soil in a 50-year maize monoculture experiment. *Plant Soil* 2022.

27. Cesarano G, Zotti M, Antignani V, Marra R, Scala F, Bonanomi G. Soil sickness and negative plant-soil feedback: A reappraisal of hypotheses. *J Plant Pathol* 2017; **99**: 545–570.

28. Jing J, Cong WF, Bezemer TM. Legacies at work: plant–soil–microbiome interactions underpinning agricultural sustainability. *Trends Plant Sci* 2022; **27**: 781–792.

29. Delavaux CS, Schemanski JL, House GL, Tipton AG, Sikes B, Bever JD. Root pathogen diversity and composition varies with climate in undisturbed grasslands, but less so in anthropogenically disturbed grasslands. *ISME J* 2021; **15**: 304–317.

30. Putten WH, Bradford MA, Pernilla Brinkman E, Voorde TFJ, Veen GF. Where, when and how plant–soil feedback matters in a changing world. *Funct Ecol* 2016; **30**: 1109–1121.

31. Raaijmakers JM, Paulitz TC, Steinberg C, Alabouvette C, Moënne-Loccoz Y. The rhizosphere: a playground and battlefield for soilborne pathogens and beneficial microorganisms. *Plant Soil* 2009; **321**: 341–361.

32. Schultz CR, Brantley KM, Wallace JG. The role of genetic variation in Zea mays response to beneficial endophytes. *Plant Growth Regul* 2022; **98**: 167–177.

33. R Core Team. R: A Language and Environment for Statistical Computing. 2021. Vienna, Austria.

34. Fox J, Weisberg S. An R Companion to Applied Regression, 3rd ed. 2019. Sage, Thousands Oaks, CA.

35. Kuznetsova A, Brockhoff PB, Christensen RHB. lmerTest Package: Tests in Linear Mixed Effects Models. *J Stat Softw* 2017; **82**.

36. Lenth R, Love J, Herve M. emmeans: Estimated Marginal Means, aka Least-Squares Means. 2020. CRAN. , https://cran.r-project.org/package=emmeans

37. Harrison XA, Donaldson L, Correa-Cano ME, Evans J, Fisher DN, Goodwin CED, et al. A brief introduction to mixed effects modelling and multi-model inference in ecology. *PeerJ* 2018; **6**: e4794.

38. Bates D, Mächler M, Bolker B, Walker S. Fitting Linear Mixed-Effects Models Using lme4. *J Stat Softw* 2015; **67**.

39. Wagner MR, Roberts JH, Balint-Kurti P, Holland JB. Heterosis of leaf and rhizosphere microbiomes in field-grown maize. *New Phytol* 2020; **228**: 1055–1069.

40. Martin M. Cutadapt removes adapter sequences from high-throughput sequencing reads. *EMBnet.journal* 2011; **17**: 10.

41. Callahan BJ, McMurdie PJ, Rosen MJ, Han AW, Johnson AJA, Holmes SP. DADA2: High-resolution sample inference from Illumina amplicon data. *Nat Methods* 2016; **13**: 581–583.

42. Wang Q, Garrity GM, Tiedje JM, Cole JR. Naïve Bayesian Classifier for Rapid Assignment of rRNA Sequences into the New Bacterial Taxonomy. *Appl Environ Microbiol* 2007; **73**: 5261–5267.

43. Callahan BJ. RDP taxonomic training data formatted for DADA2 (RDP trainset 16/release 11.5). 2017. Zenodo.

44. UNITE Community. UNITE general FASTA release. 2017.

45. McMurdie PJ, Holmes S. phyloseq: An R Package for Reproducible Interactive Analysis and Graphics of Microbiome Census Data. *PLoS One* 2013; **8**: e61217.

46. Fernandes AD, Reid JNS, Macklaim JM, McMurrough TA, Edgell DR, Gloor GB. Unifying the analysis of high-throughput sequencing datasets: characterizing RNA-seq, 16S rRNA gene sequencing and selective growth experiments by compositional data analysis. *Microbiome* 2014; **2**: 15.

47. Gloor GB, Macklaim JM, Pawlowsky-Glahn V, Egozcue JJ. Microbiome Datasets Are Compositional: And This Is Not Optional. *Front Microbiol* 2017; **8**: 1–6.

48. Oksanen J, Guillaume Blanchet F, Friendly M, Kindt R, Legendre P, McGlinn D, et al. vegan: Community Ecology Package. 2019.

49. Benjamini Y, Hochberg Y. Controlling the False Discovery Rate : A Practical and Powerful Approach to Multiple Testing. *J R Stat Soc* 1995; **57**: 289–300.

50. Kuhn M. Building Predictive Models in R Using the caret Package. *J Stat Softw* 2008; **28**: 159–160.

51. Wright MN, Ziegler A. ranger : A Fast Implementation of Random Forests for High Dimensional Data in C++ and R. *J Stat Softw* 2017; **77**.

52. Bertness MD, Callaway R. Positive interactions in communities. *Trends Ecol Evol* 1994; **9**: 191–193.

53. Sharp RE, Davies WJ. Solute regulation and growth by roots and shoots of water-stressed maize plants. *Planta* 1979; **147**: 43–49.

54. Lynch JP, Chimungu JG, Brown KM. Root anatomical phenes associated with water acquisition from drying soil: Targets for crop improvement. *J Exp Bot* 2014; **65**: 6155–6166.

55. Gao Y, Lynch JP. Reduced crown root number improves water acquisition under water deficit stress in maize (Zea mays L.). *J Exp Bot* 2016; **67**: 4545–4557.

56. Zhan A, Schneider H, Lynch JP. Reduced Lateral Root Branching Density Improves Drought Tolerance in Maize. *Plant Physiol* 2015; **168**: 1603–1615.

57. Sebastian J, Yee M-C, Goudinho Viana W, Rellán-Álvarez R, Feldman M, Priest HD, et al. Grasses suppress shoot-borne roots to conserve water during drought. *Proc Natl Acad Sci* 2016; **113**: 8861–8866.

58. Manzoni S, Schimel JP, Porporato A. Responses of soil microbial communities to water stress: results from a meta-analysis. *Ecology* 2012; **93**: 930–938.

59. Henry A, Doucette W, Norton J, Bugbee B. Changes in Crested Wheatgrass Root Exudation Caused by Flood, Drought, and Nutrient Stress. *J Environ Qual* 2007; **36**: 904–912.

60. Preece C, Peñuelas J. Rhizodeposition under drought and consequences for soil communities and ecosystem resilience. *Plant Soil* 2016; **409**: 1–17.

61. Karlowsky S, Augusti A, Ingrisch J, Hasibeder R, Lange M, Lavorel S, et al. Land use in mountain grasslands alters drought response and recovery of carbon allocation and plant-microbial interactions. *J Ecol* 2018; **106**: 1230–1243.

62. Svenningsson H, Sundin P, Liljenberg C. Lipids, carbohydrates and amino acids exuded from the axenic roots of rape seedlings exposed to water-deficit stress. *Plant, Cell Environ* 1990; **13**: 155–162.

63. Canarini A, Merchant A, Dijkstra FA. Drought effects on Helianthus annuus and Glycine max metabolites: from phloem to root exudates. *Rhizosphere* 2016; **2**: 85–97.

64. Calvo OC, Franzaring J, Schmid I, Müller M, Brohon N, Fangmeier A. Atmospheric CO 2 enrichment and drought stress modify root exudation of barley. *Glob Chang Biol* 2017; **23**: 1292–1304.

65. Zhalnina K, Louie KB, Hao Z, Mansoori N, da Rocha UN, Shi S, et al. Dynamic root exudate chemistry and microbial substrate preferences drive patterns in rhizosphere microbial community assembly. *Nat Microbiol* 2018; **3**: 470–480.

66. Xu L, Dong Z, Chiniquy D, Pierroz G, Deng S, Gao C, et al. Genome-resolved metagenomics reveals role of iron metabolism in drought-induced rhizosphere microbiome dynamics. *Nat Commun* 2021; **12**: 3209.

67. Furze JR, Martin AR, Nasielski J, Thevathasan N V., Gordon AM, Isaac ME. Resistance and resilience of root fungal communities to water limitation in a temperate agroecosystem. *Ecol Evol* 2017; **7**: 3443–3454.

68. de Vries FT, Liiri ME, Bjørnlund L, Bowker MA, Christensen S, Setälä HM, et al. Land use alters the resistance and resilience of soil food webs to drought. *Nat Clim Chang* 2012; **2**: 276–280.

69. Griffin DM. A comparison of the roles of bacteria and fungi, Volume 1: *Bacteria in Nature* . 1985. Springer US, Boston, MA.

70. Wyatt TT, Wösten HAB, Dijksterhuis J. Fungal Spores for Dispersion in Space and Time. *Advances in Applied Microbiology*. 2013. pp 43–91.

71. Harris RF. Effect of Water Potential on Microbial Growth and Activity. In: Parr JF, Gardner WR, Elliott LF (eds). *Water Potential Relations in Soil Microbiology*, 9th ed. 1981. Soil

Science Society of America, Madison W.I., pp 23–95.

72. Schimel J, Balser TC, Wallenstein M. Microbial stress-response physiology and its implications for ecosystem function. *Ecology* 2007; **88**: 1386–1394.

73. Schimel JP, Scott WJ, Killham K. Changes in Cytoplasmic Carbon and Nitrogen Pools in a Soil Bacterium and a Fungus in Response to Salt Stress. *Appl Environ Microbiol* 1989; **55**: 1635–1637.

74. Killham K, Firestone MK. Salt stress control of intracellular solutes in streptomycetes indigenous to saline soils. *Appl Environ Microbiol* 1984; **47**: 301–306.

75. Neilson JW, Califf K, Cardona C, Copeland A, van Treuren W, Josephson KL, et al. Significant Impacts of Increasing Aridity on the Arid Soil Microbiome. *mSystems* 2017; **2**.

76. Araya JP, González M, Cardinale M, Schnell S, Stoll A. Microbiome Dynamics Associated With the Atacama Flowering Desert. *Front Microbiol* 2020; **10**: 1–13.

77. Wan X, Chen X, Huang Z, Chen HYH. Global soil microbial biomass decreases with aridity and land-use intensification. *Glob Ecol Biogeogr* 2021; **30**: 1056–1069.

78. Hooper DU, Chapin FS, Ewel JJ, Hector A, Inchausti P, Lavorel S, et al. Effects of biodiversity on ecosystem functioning: A consensus of current knowledge. *Ecol Monogr* 2005; **75**: 3–35.

79. Delgado-Baquerizo M, Guerra CA, Cano-Díaz C, Egidi E, Wang JT, Eisenhauer N, et al. The proportion of soil-borne pathogens increases with warming at the global scale. *Nat Clim Chang* 2020; **10**: 550–554.

80. Větrovský T, Kohout P, Kopecký M, Machac A, Man M, Bahnmann BD, et al. A meta-analysis of global fungal distribution reveals climate-driven patterns. *Nat Commun* 2019; **10**: 1–9.

81. Chen QL, Hu HW, Yan ZZ, Li CY, Nguyen BAT, Zhu YG, et al. Precipitation increases the abundance of fungal plant pathogens in Eucalyptus phyllosphere. *Environ Microbiol* 2021; **23**: 7688–7700.

82. Beals KK, Moore JAM, Kivlin SN, Bayliss SLJ, Lumibao CY, Moorhead LC, et al. Predicting plant-soil feedback in the field: Meta-analysis reveals that competition and environmental stress differentially influence psf. *Front Ecol Evol* 2020; **8**.

83. Veresoglou SD, Li GC, Chen J, Johnson D. Direction of plant–soil feedback determines plant responses to drought. *Glob Chang Biol* 2022; **28**: 3995–3997.

84. Hassan K, Carrillo Y, Nielsen UN. The effect of prolonged drought legacies on plant–soil feedbacks. *J Veg Sci* 2021; **32**: 1–17.

85. Lozano YM, Aguilar-Trigueros CA, Ospina JM, Rillig MC. Drought legacy effects on root

morphological traits and plant biomass via soil biota feedback. *New Phytol* 2022; **236**: 222–234.

86. Bennett AJ, Bending GD, Chandler D, Hilton S, Mills P. Meeting the demand for crop production: the challenge of yield decline in crops grown in short rotations. *Biol Rev* 2012; **87**: 52–71.

87. Wang G, Bei S, Li J, Bao X, Zhang J, Schultz PA, et al. Soil microbial legacy drives crop diversity advantage: Linking ecological plant–soil feedback with agricultural intercropping. *J Appl Ecol* 2021; **58**: 496–506.

88. Peralta AL, Sun Y, McDaniel MD, Lennon JT. Crop rotational diversity increases disease suppressive capacity of soil microbiomes. *Ecosphere* 2018; **9**.

89. Zhang BQ, Chen WD, Yang XB. Occurrence of Pythium species in long-term maize and soybean monoculture and maize/soybean rotation. *Mycol Res* 1998; **102**: 1450–1452.

90. Vik U, Logares R, Blaalid R, Halvorsen R, Carlsen T, Bakke I, et al. Different bacterial communities in ectomycorrhizae and surrounding soil. *Sci Rep* 2013; **3**: 3471.

91. Stafford WHL, Baker GC, Brown SA, Burton SG, Cowan DA. Bacterial diversity in the rhizosphere of Proteaceae species. *Environ Microbiol* 2005; **7**: 1755–1768.

92. Zhang Q, Acuña JJ, Inostroza NG, Duran P, Mora ML, Sadowsky MJ, et al. Niche Differentiation in the Composition, Predicted Function, and Co-occurrence Networks in Bacterial Communities Associated With Antarctic Vascular Plants. *Front Microbiol* 2020; **11**: 1–13.

93. Dye DW, Kemp WJ. A taxonomic study of plant pathogenic Corynebacterium species. *New Zeal J Agric Res* 1977; **20**: 563–582.

94. Vidaver AK, Mandel M. Corynebacterium nebraskense, a New, Orange-Pigmented Phytopathogenic Species. *Int J Syst Bacteriol* 1974; **24**: 482–485.

95. Panke-Buisse K, Poole AC, Goodrich JK, Ley RE, Kao-Kniffin J. Selection on soil microbiomes reveals reproducible impacts on plant function. *ISME J* 2015; **9**: 980–989.

96. Huang K, Sun X, Zou Y, Li H, Xu P, Zhang W, et al. Comparison of the Endophytic Bacterial Microbiota of Asymptomatic and Symptomatic Ginger Rhizomes During the Activation of Adventitious Bud Development. *Plant Dis* 2022; **106**: 2470–2479.

97. Wang X, Shi W, Wang J, Gao Z, Li S, Wang N, et al. Control of Southern Root-knot Nematodes on Tomato and Regulation of Soil Bacterial Community by Biofumigation with Zanthoxylum bungeanum Seed. *Hortic Plant J* 2021; **7**: 49–58.

98. Chuah L-O, Yap K-P, Thong KL, Liong MT, Ahmad R, Shamila-Syuhada AK, et al. Genome Sequence of “Anthococcus,” a Novel Genus of the Family Streptococcaceae Isolated from Flowers. *Genome Announc* 2016; **4**.

99. Yu AO, Leveau JHJ, Marco ML. Abundance, diversity and plant-specific adaptations of plant-associated lactic acid bacteria. *Environ Microbiol Rep* 2020; **12**: 16–29.

100. Minervini F, Celano G, Lattanzi A, Tedone L, De Mastro G, Gobbetti M, et al. Lactic Acid Bacteria in Durum Wheat Flour Are Endophytic Components of the Plant during Its Entire Life Cycle. *Appl Environ Microbiol* 2015; **81**: 6736–6748.

Figures

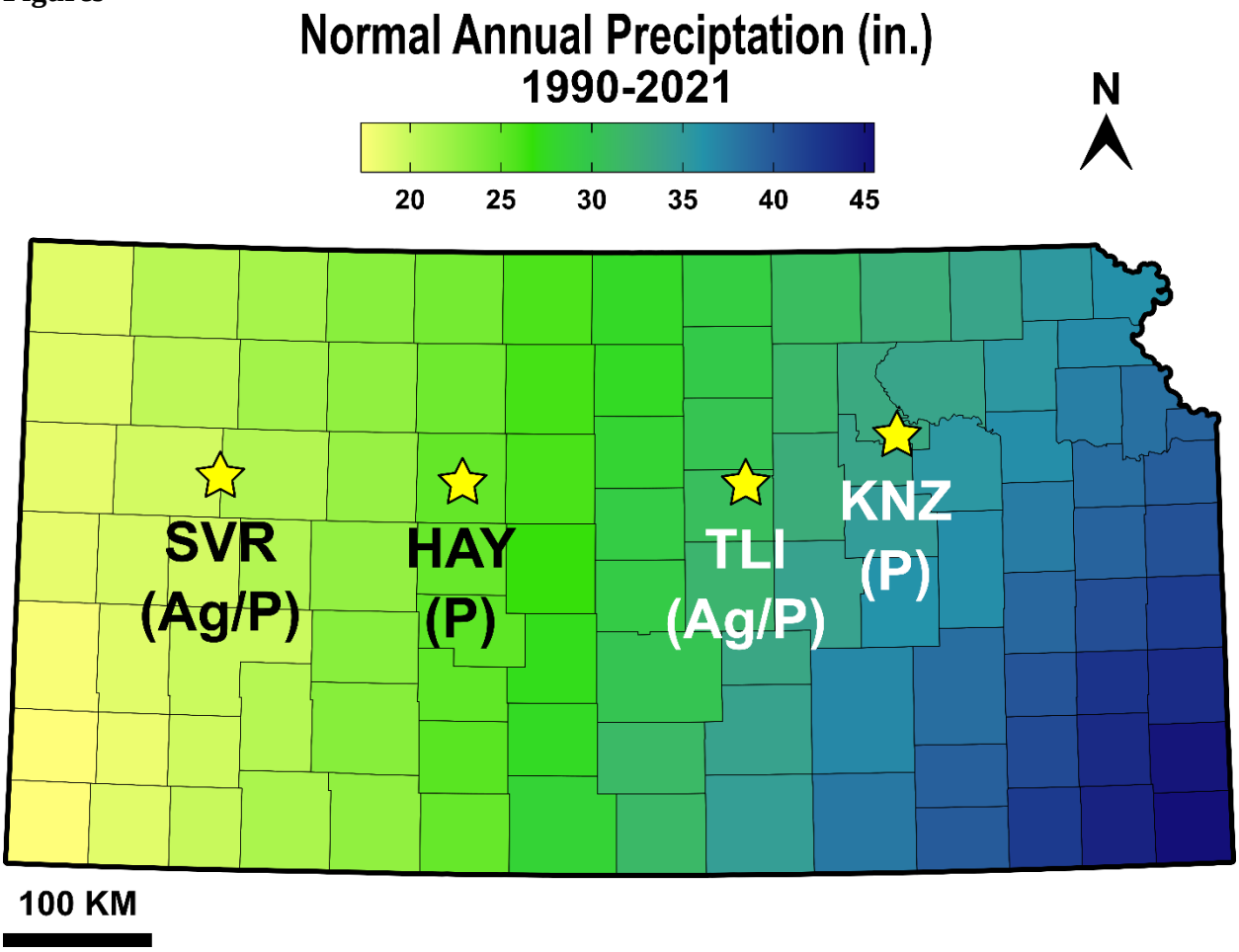

Figure 1. Kansas precipitation gradient. Soil samples were collected from either agricultural grain fields (Ag) or native prairies (P) (land use types) at four locations in Kansas along an increasing precipitation gradient (Smoky Valley Ranch [SVR] prairie [latitude 38.8665, longitude -100.9951], SVR grain field [38.8791, -100.9828], Hayes [HAY] prairie [38.8355, -99.3033], The Land Institute [TLI] grain field [38.6943, -97.5912], TLI prairie [38.9698, -97.4690], and Konza [KNZ] native prairie [39.1056, -96.6099]).

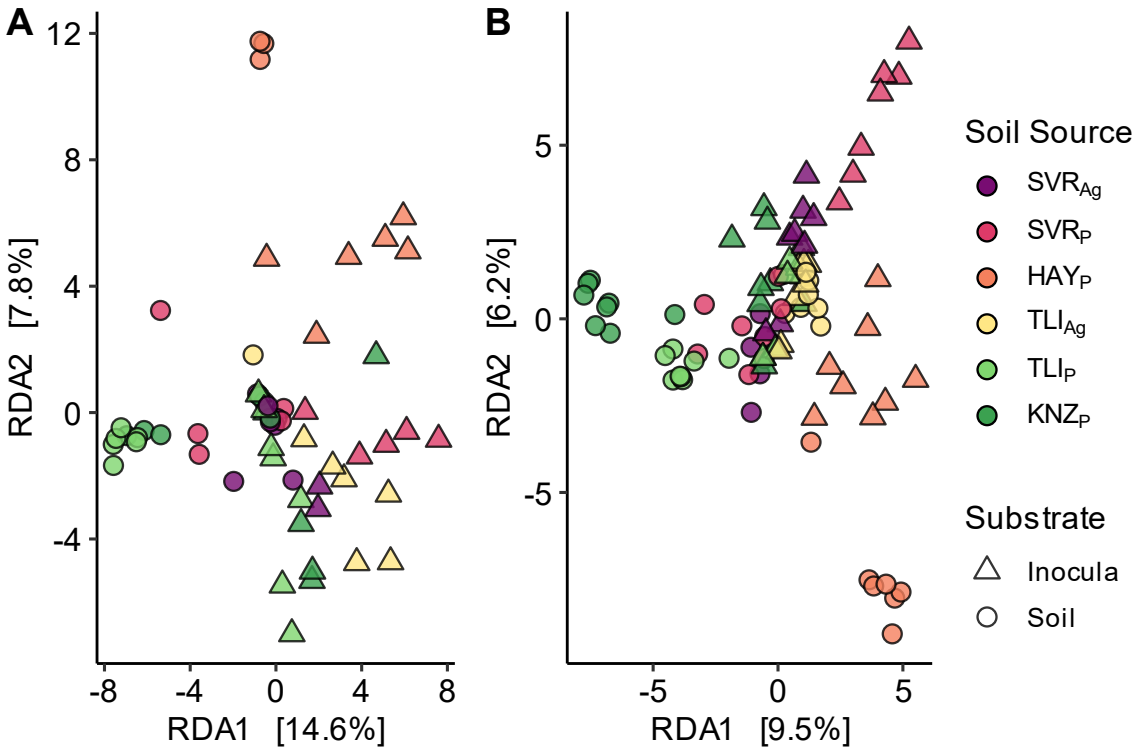

Figure 2. Soil community composition is strongly differentiated across the soil sources and substrates. Redundancy analysis for **A**) bacterial and **B**) fungal communities from soil sources used to derive soil inocula. Soil source and substrate are represented by differing colors or shapes, respectively.

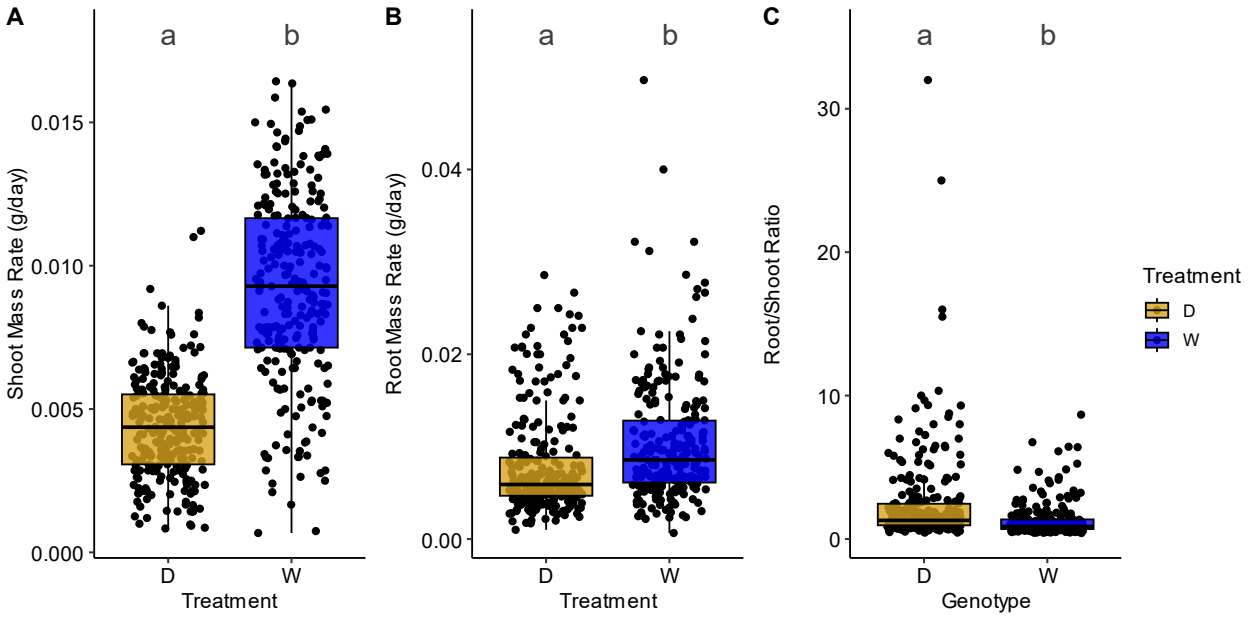

Figure 3. Shoot and root growth vary across drought treatment. The effect of drought treatment on **A)** shoot mass rate, **B)** root mass rate, and **C)** root/shoot ratio. Boxplot hinges represent the 1st and 3rd quartiles; whiskers represent 1.5 times the interquartile range; letters above box plots denote significant differences in estimated marginal means (*p*-value=<0.01; see Table 1 for full ANOVA table).

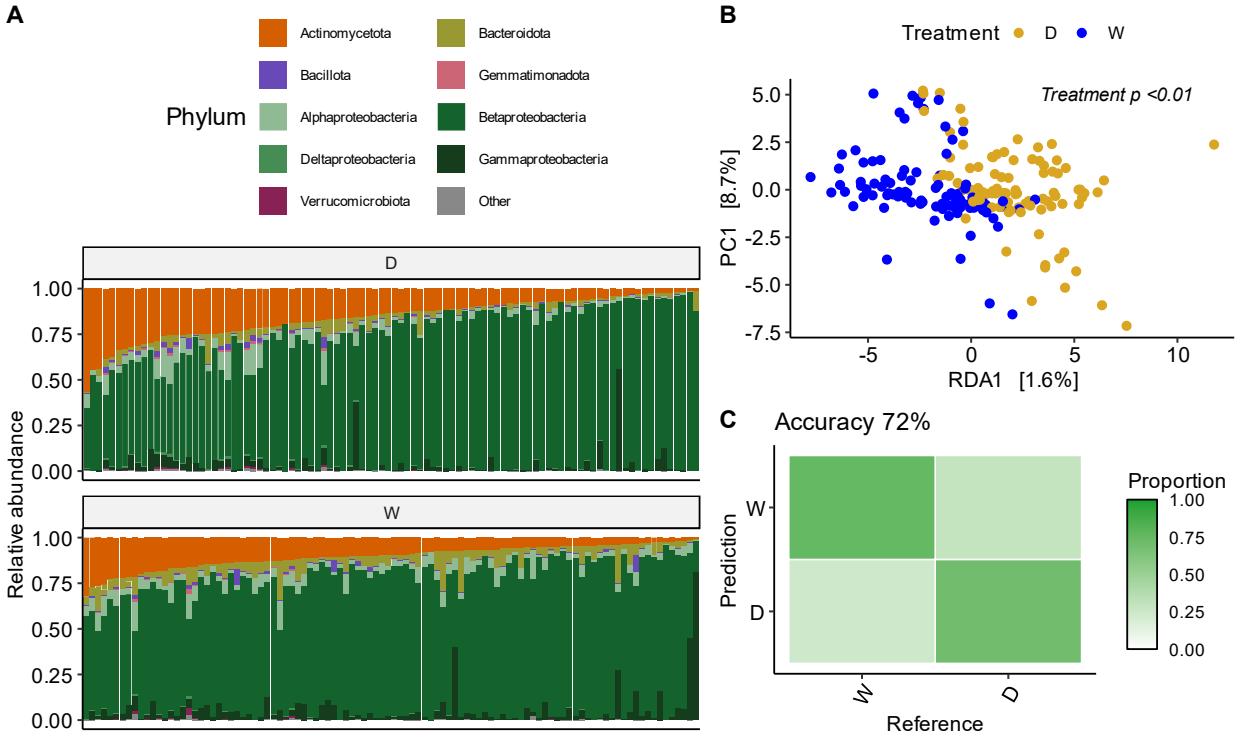

Figure 4. Bacterial community composition across drought treatment. A) Bacterial and taxonomic barplots for drought (D) and well-watered (W) plants. Each sample is represented by a single line with the relative abundance (non CLR transformed data) of each phylum displayed by color. **B)** Redundancy analysis on bacterial communities fit by drought treatment. Redundancy analysis was conditioning for sequencing batch and log transformed usable reads per sample. **C)** Confusion matrix depicting the classification accuracy of a random forest classifier predicting drought treatment trained on bacterial communities. Above the confusion matrix balanced accuracy is shown, for additional classifier statistics see Table S8

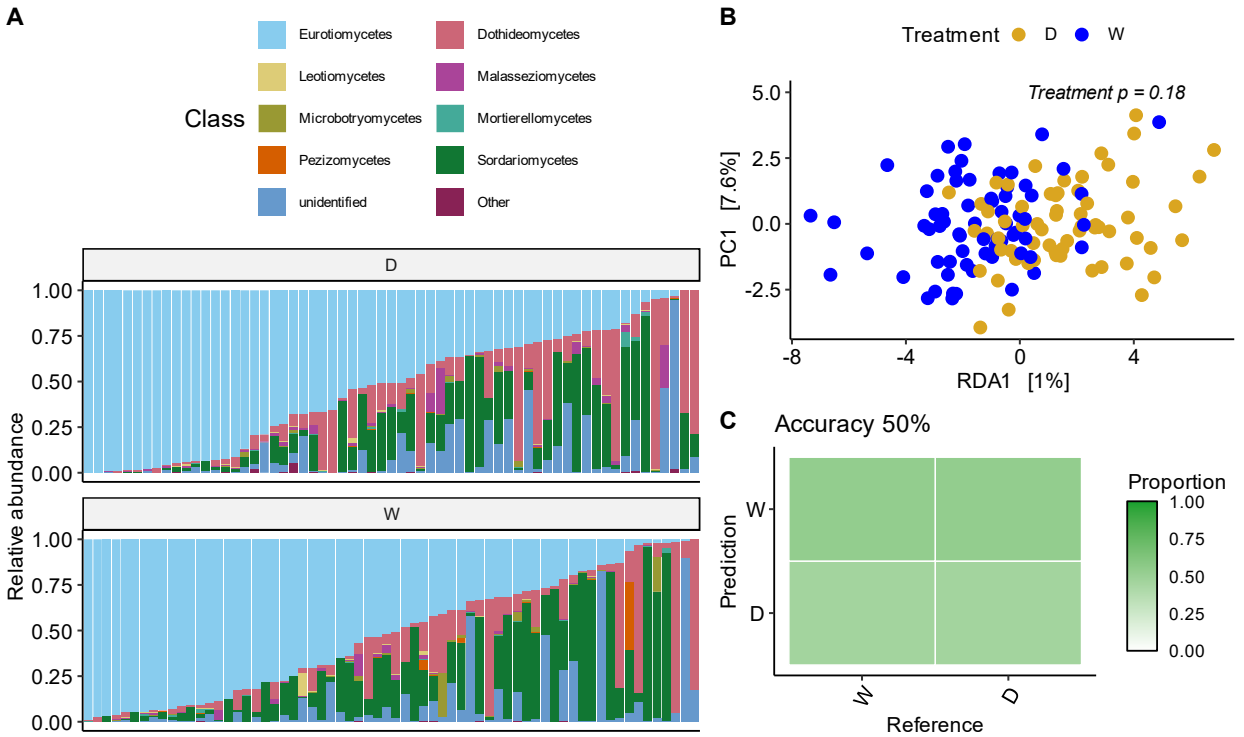

Figure 5. Fungal community composition across drought treatment. A) Fungal taxonomic barplots for drought (D) and well-watered (W) plants. Each sample is represented by a single line with the relative abundance (non CLR transformed data) of each class displayed by color. **B)** Redundancy analysis on fungal communities fit by drought treatment. Redundancy analysis was conditioning for sequencing batch and log transformed usable reads per sample. **C)** Confusion matrix depicting the classification accuracy of random forest a classifier predicting drought treatment trained on fungal communities. Above the confusion matrix balanced accuracy is shown, for additional classifier statistics see Table S9.

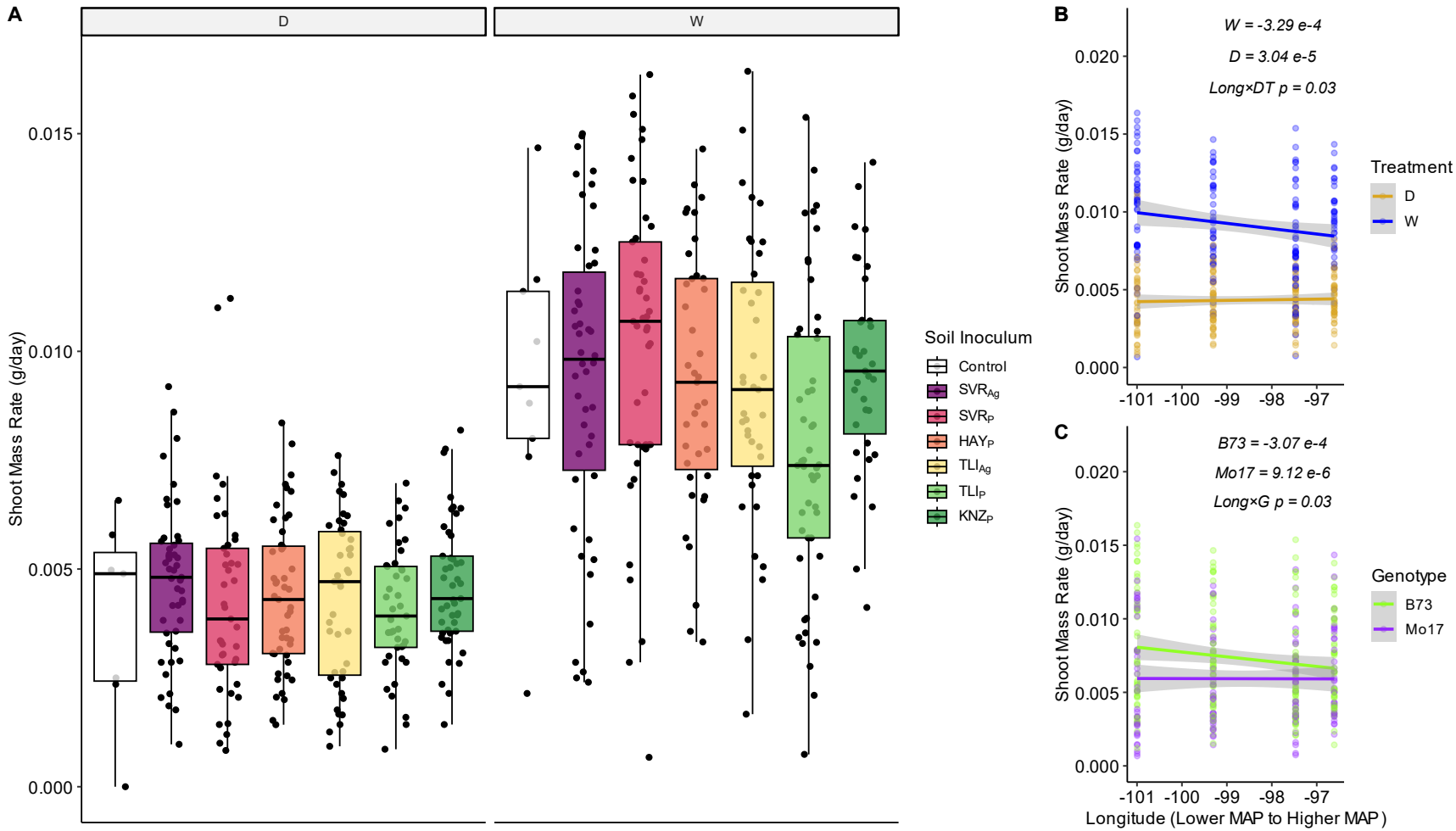

Figure 6. Shoot mass accumulation rate by soil inoculum. Boxplots are colored by soil inoculum for **A)** shoot mass rate. Separate facets represent drought (D) and well-watered plants (W). Boxplot hinges represent the 1st and 3rd quartiles; whiskers represent 1.5 times the interquartile range. **B-C)** trend lines for shoot mass rate of significant interactions of longitude (Long) with drought treatment and genotype, respectively, for plants inoculated with prairie soils.

Tables

Table 1. Type three analysis of variance (ANOVA) for plant growth responses.

		sqrt(Shoot mass rate)		sqrt(Root Mass Rate)		log(Root/shoot Ratio)	
Factor	DF	*F*-value	*p*-value	*F*-value	*p*-value	*F*-value	*p*-value
Drought Treatment (DT)	1	471.39	**<0.01**	31.09	**<0.01**	216.09	**<0.01**
Genotype (G)	1	32.57	**<0.01**	30.34	**<0.01**	111.01	**<0.01**
Soil Inoculum (SI)	5	3.42	**<0.01**	0.4	0.85	2.14	0.06
DT x G	1	0.11	0.74	2.36	0.12	0.15	0.7
DT x SI	5	1.3	0.26	1.18	0.32	0.99	0.42
G x SI	5	1.95	0.09	0.64	0.67	2.65	**0.02**
DT x G x SI	5	0.77	0.57	0.22	0.95	0.12	0.99

Bold values denote significant effects, *p*-value<0.05

Table 2. Permutational Multivariate ANOVA (PERMANOVA) table bacterial community composition of maize nodal roots.

Factor	DF	SS	R^2	*F*-value	*p*-value
Genotype (G)	1	4109	0.01	1.23	0.21
Soil Inoculum (SI)	5	34055	0.05	2.04	**<0.01**
Drought Treatment (DT)	1	7483	0.01	2.24	**<0.01**
SI x DT	5	16011	0.02	0.96	0.52
Residual	185	617812	0.91		

Bold values denote significant effects, *p*-value<0.05

Table 3. PERMANOVA table for fungal community composition of maize nodal roots.

Factor	DF	SS	R^2	*F*-value	*p*-value
Genotype (G)	1	774	0.01	1.01	0.28
Soil Inoculum (SI)	5	9152	0.09	2.40	**<0.01**
Drought Treatment (DT)	1	693	0.01	0.91	0.42
SI x DT	5	4198	0.04	1.10	0.22
Residual	116	88478	0.86		

Bold values denote significant effects, *p*-value<0.05

Table 4. Bacterial families associated with square root transformed shoot mass rate.

Taxon	Model Term	R	X	PVE_{Res}	Rel. Abund.	*q*
Lactobacillaceae	Abundance	3.92E-04	-1.52E-02	3.6	0.14	3.78E-04
Nocardiaceae	Abundance	2.84E-04	-1.43E-02	3.63	0.02	4.78E-04
Microbacteriaceae	Abundance	1.11E-04	-1.51E-02	5.14	1.17	3.04E-05
Sinobacteraceae	Abundance	1.03E-04	-1.46E-02	2.31	0.05	4.81E-03
Micrococcaceae	Abundance	2.58E-05	-1.48E-02	2.77	8.06	2.21E-03
Alcaligenaceae	Abundance	1.58E-06	-1.42E-02	3.04	0.05	1.39E-03
Corynebacteriaceae*	Abundance	-1.19E-04	-1.40E-02	6.38	0.01	7.67E-07
Sphingomonadaceae	Abundance	-1.21E-04	-1.25E-02	5.49	1.18	1.98E-05
Streptococcaceae*	Abundance	-1.61E-04	-1.39E-02	5.52	0.02	7.59E-06
Rhodospirillaceae	Abundance	-4.46E-04	-1.19E-02	5.54	0.08	1.75E-05
Dietziaceae	Abundance	-6.54E-04	-1.38E-02	4.97	<0.01	2.43E-05
Beijerinckiaceae	Abundance	-8.49E-04	-1.46E-02	2.76	<0.01	2.19E-03
Actinomycetaceae	Abundance	-1.85E-03	-1.47E-02	2.18	<0.01	5.79E-03

*Corynebacteriaceae and Streptococcaceae both show significant interactions between the family abundance and drought treatment, these are presented in Figure S11.

Table 5. Fungal orders associated with square root transformed shoot mass rate.

Taxon	Trait	Model Term	R	X	PVE_{Res}	Relative Abundance	*q*
Hypocreales	SMR	Abundance	4.75E-05	-1.42E-02	3.28	19.23	0.01
Malasseziales	SMR	Abundance	9.97E-05	-1.42E-02	2.92	1.22	0.01
Sporidiobolales	SMR	Abundance	6.36E-04	-1.34E-02	4.87	0.66	0.00

Supplemental Figures

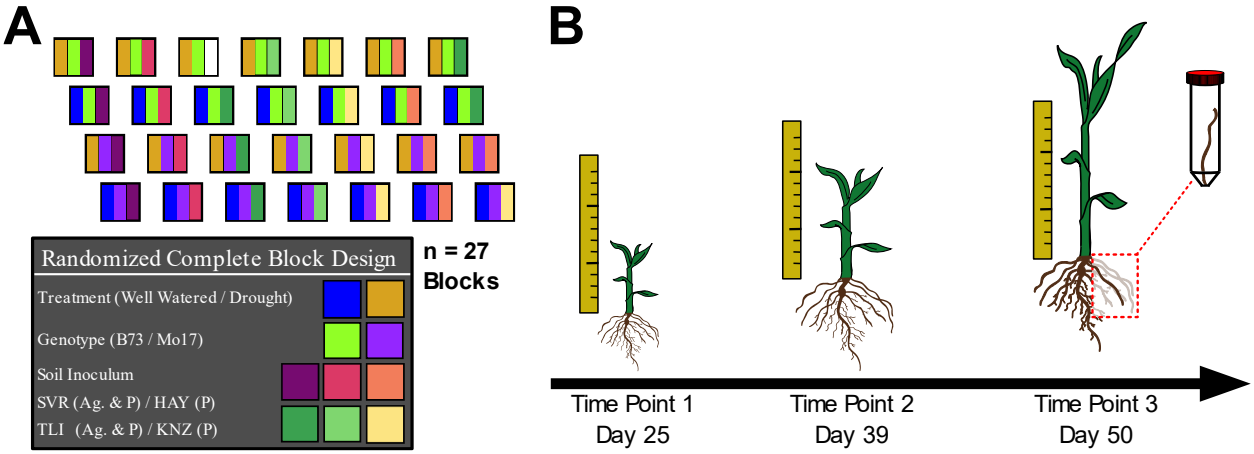

Figure S1. Experimental design. A) A complete randomized block design (blocks=27) was used. Each pot was filled with sterile calcined clay soil mix and received a seed of either *Zea mays* genotype B73 or Mo17, was subject to either well-watered or drought conditions, and was inoculated with one of the six inocula. One uninoculated control was used per randomized block (denoted with white stripe). **B)** Plant biomass was collected in a time series: for time point one (day 25) and two (day 39), 100 plants each were destructively harvested, then dried for root and shoot biomass. For the third time point (day 50), all remaining plants (n=529 – non-germinates) were harvested. Prior to drying for biomass measures, one nodal root from each plant was collected for amplicon sequencing for bacterial and fungal microbiome composition.

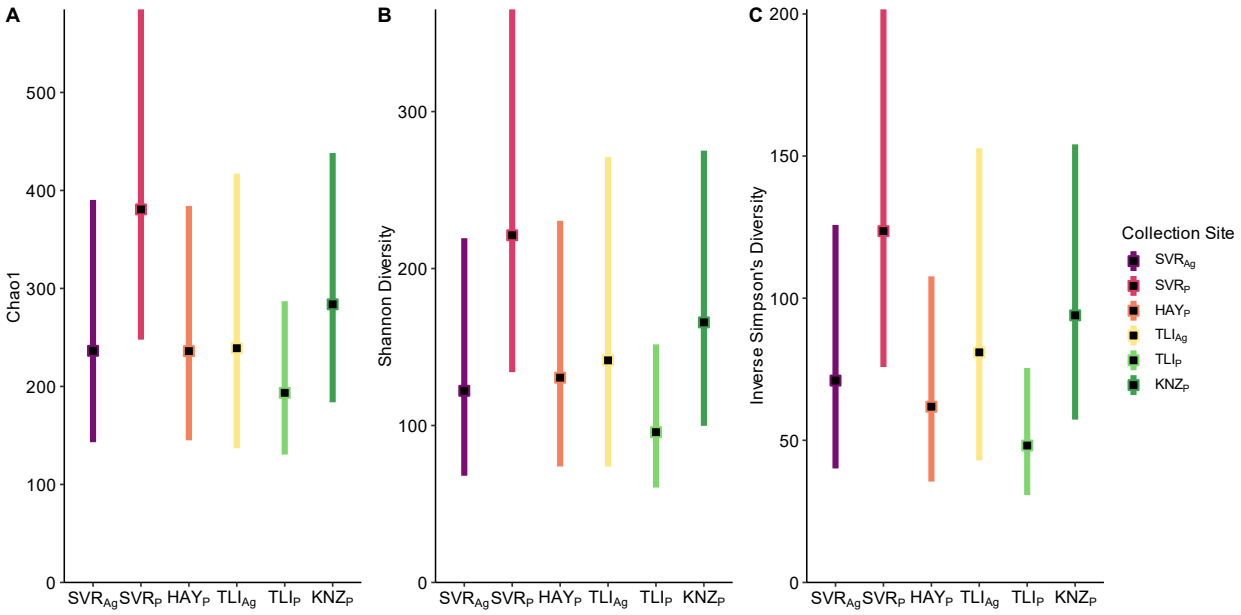

Figure S2. Bacterial alpha diversity values for **A)** Chao1 **B)** Shannon Diversity and **C)** Inverse Simpson's Diversity. Black squares represent estimated marginal means (EMM) for each collection site and colored bars show the 95% confidence intervals for the EMMs.

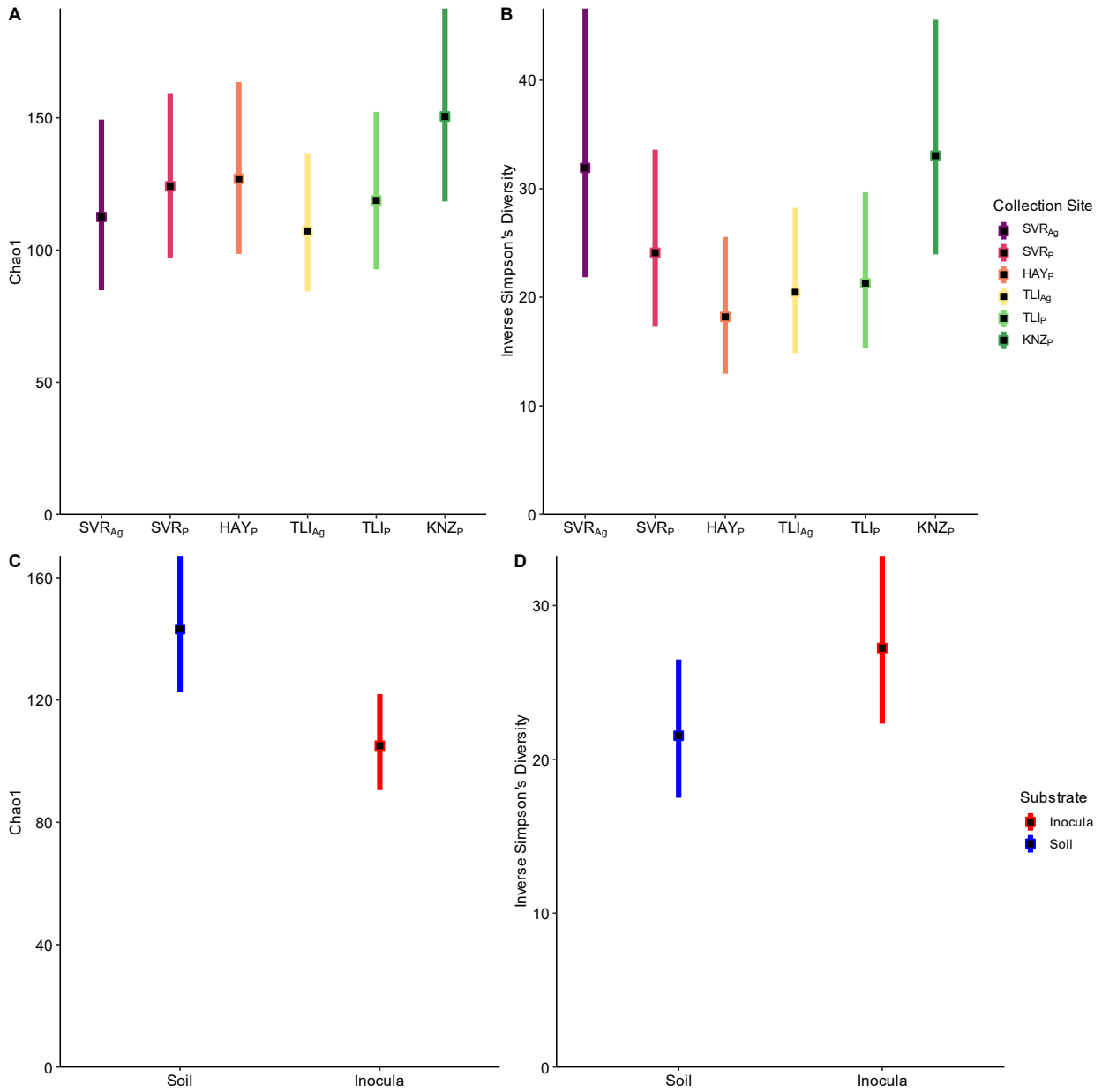

Figure S3. Fungal alpha diversity values for **A/C)** Chao1 and **B/D)** Inverse Simpson's Diversity. Black squares represent estimated marginal means (EMM) for each collection site or substrate and colored bars show the 95% confidence intervals for the EMMs.

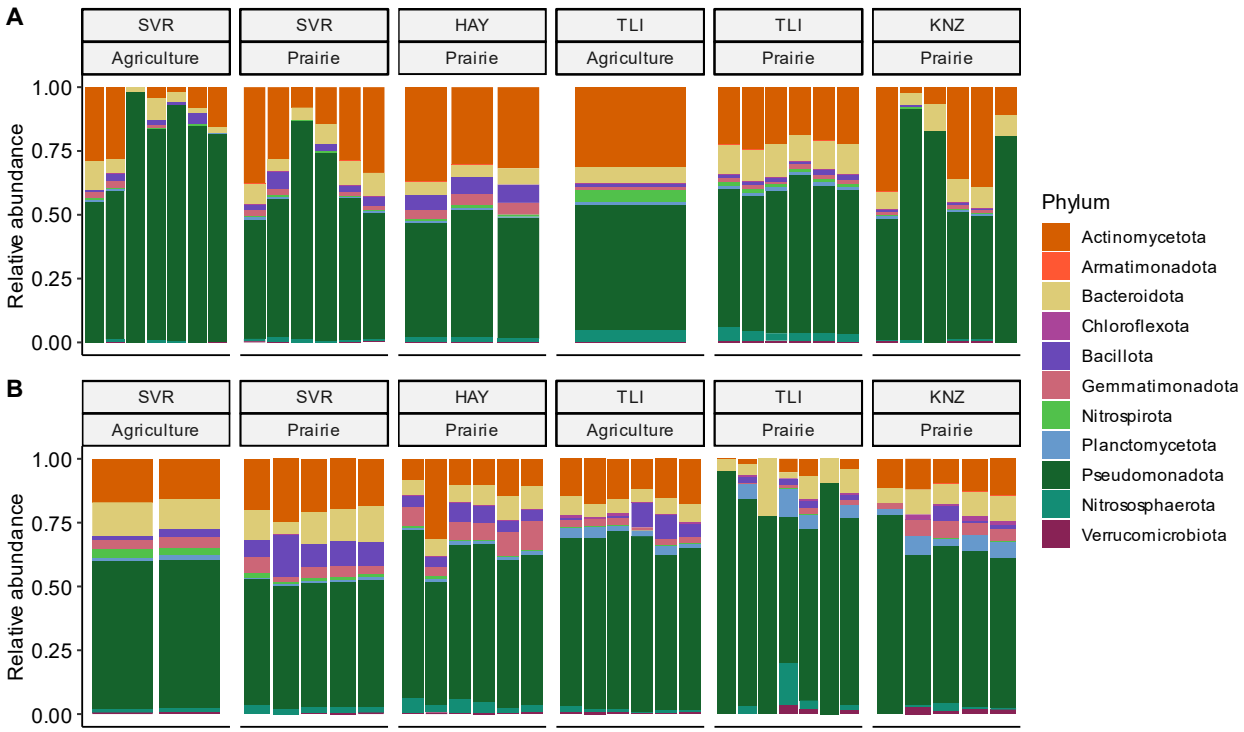

Figure S4. Taxonomic bar plots for bacterial phyla for **A)** soil and **B)** inocula samples. Historical annual precipitation for each collection site (SVR, HAY, TLI, KNZ) increases from left to right. Each sample is represented by a single line with the relative abundance (non CLR transformed data) of each phylum displayed by color.

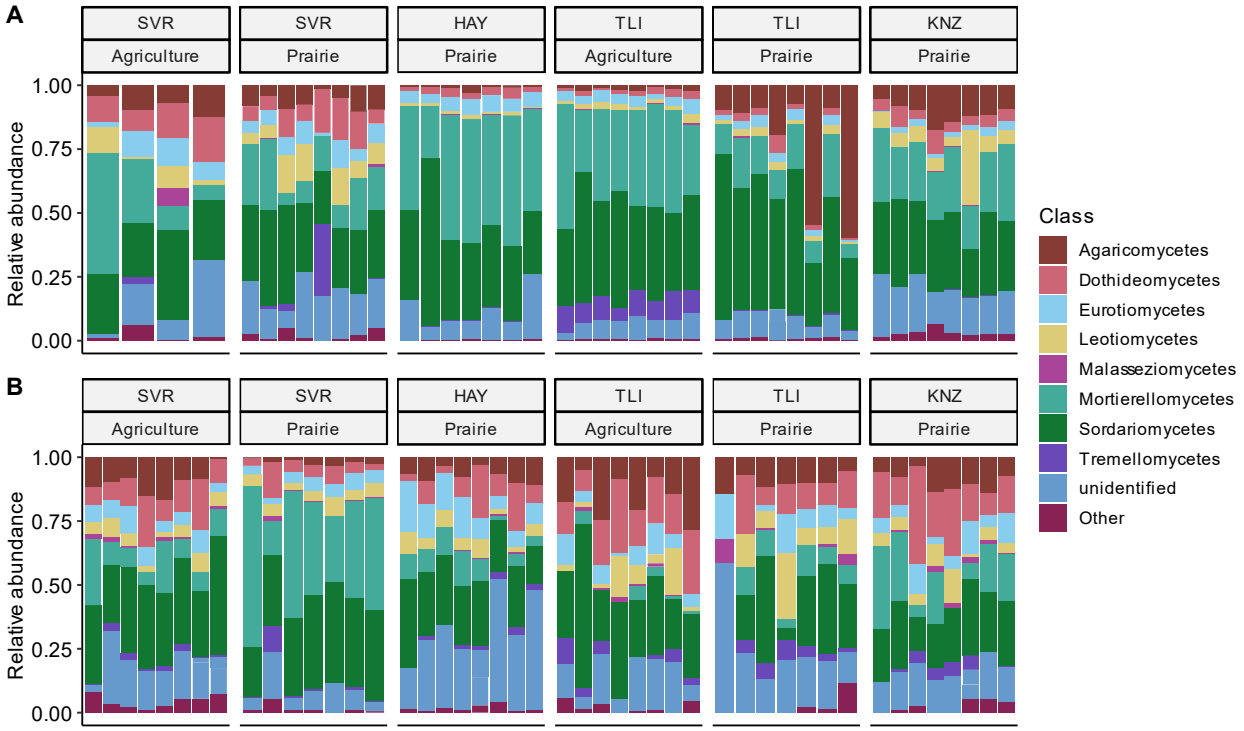

Figure S5. Taxonomic bar plots for fungal classes for **A)** soil and **B)** inocula samples. Historical annual precipitation for each collection site (SVR, HAY, TLI, KNZ) increases from left to right. Each sample is represented by a single line with the relative abundance (non CLR transformed data) of each class displayed by color.

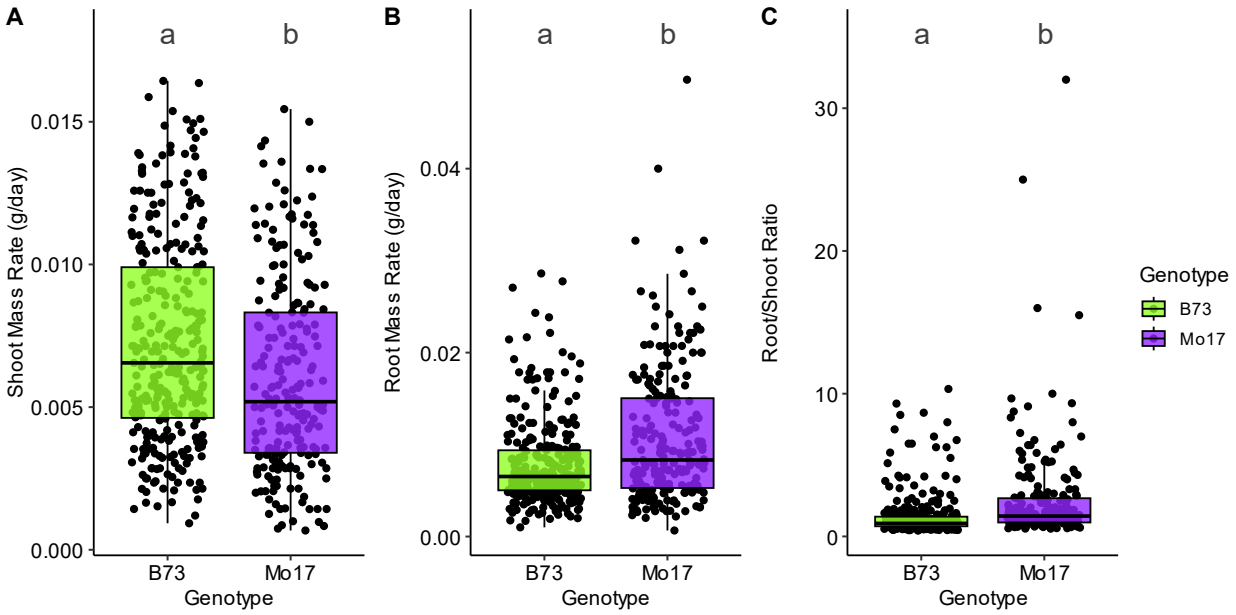

Figure S6. Maize genotypes growth differs across **A)** shoot mass rate, **B)** root mass rate, and **C)** root/shoot ratio. Boxplot hinges represent the 1st and 3rd quartiles; whiskers represent 1.5 times the interquartile range; letters above box plots denote significant differences in estimated marginal means (*p*-value=<0.01; see Table 1 for full ANOVA table).

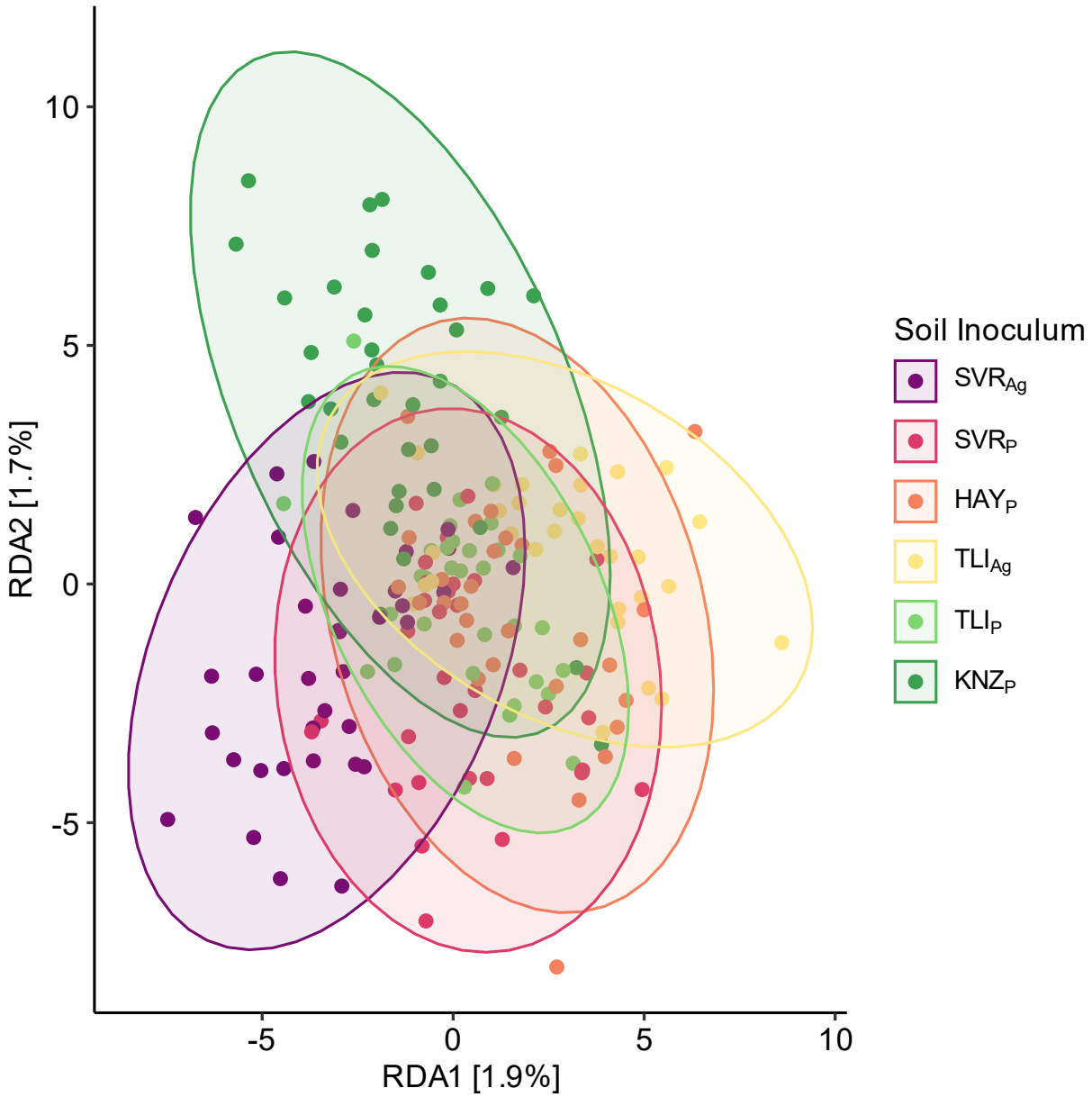

Figure S7. Redundancy analysis for root bacterial community composition. Points are colored by soil inoculum. Normal data ellipses are colored by soil inoculum assuming a multivariate normal distribution.

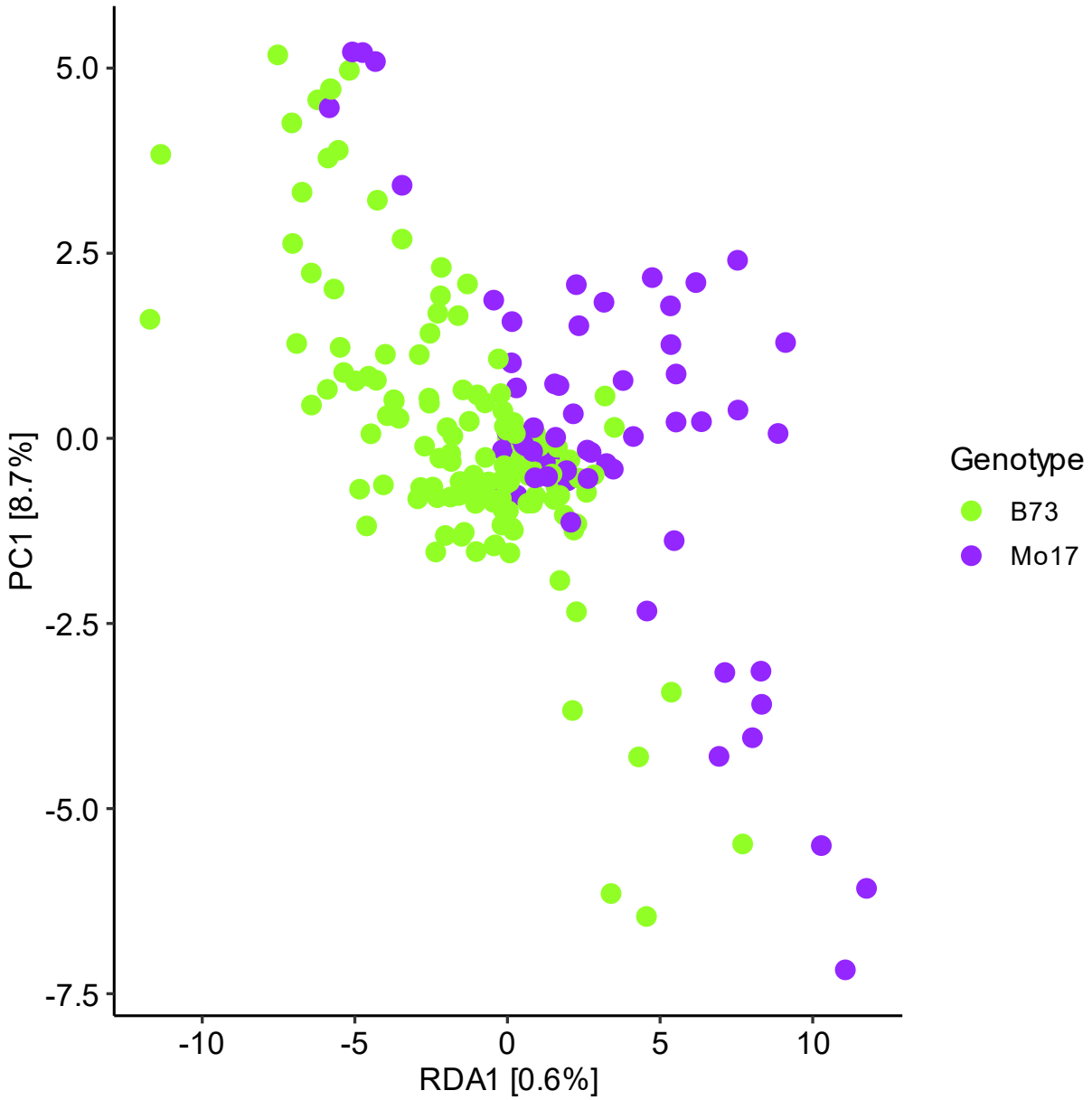

Figure S8. Redundancy analysis for root bacterial community composition. Points are colored by maize genotype.

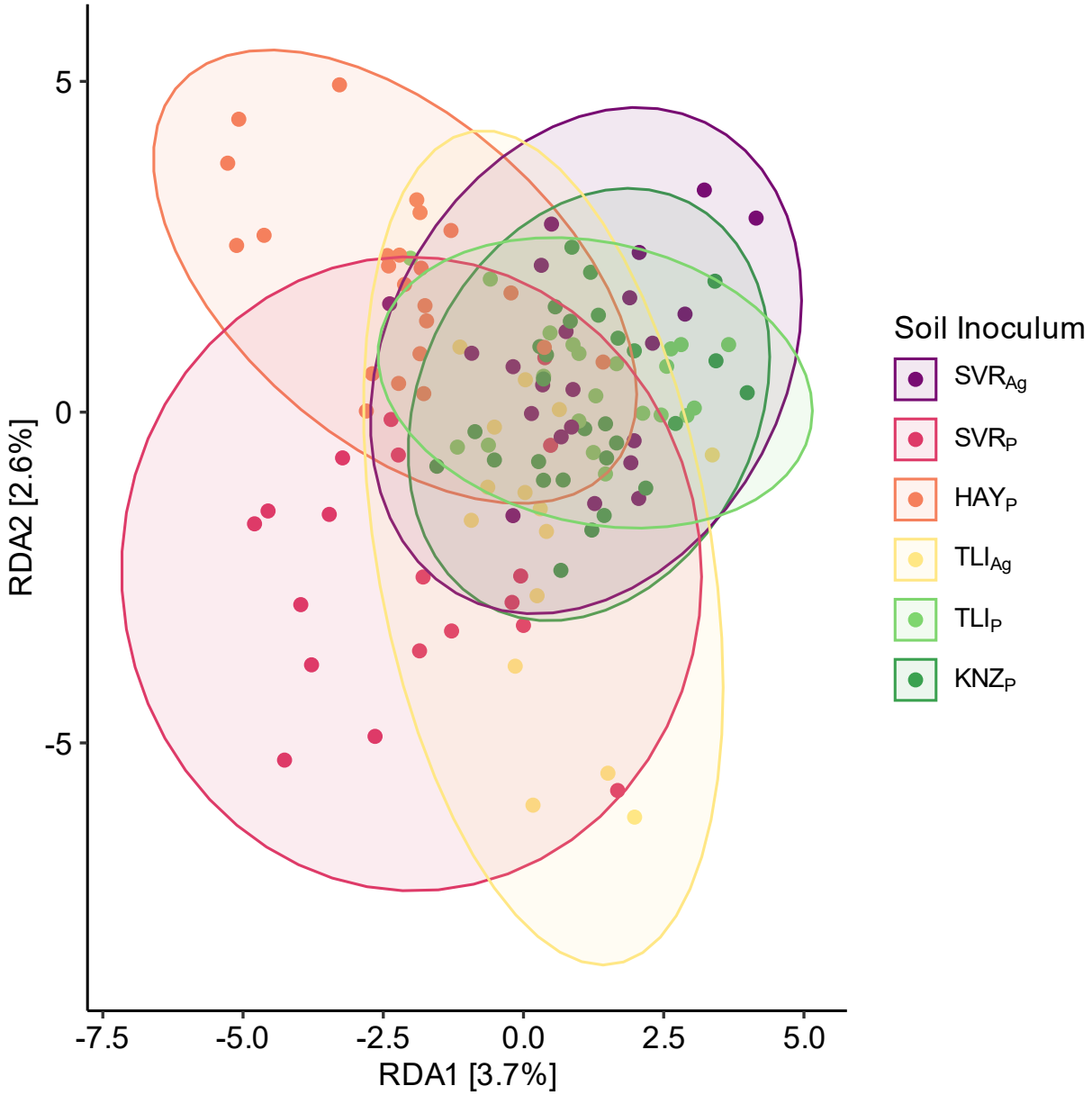

Figure S9. Redundancy analysis for root fungal community composition. Points are colored by soil inoculum. Normal data ellipses are colored by soil inoculum assuming a multivariate normal distribution.

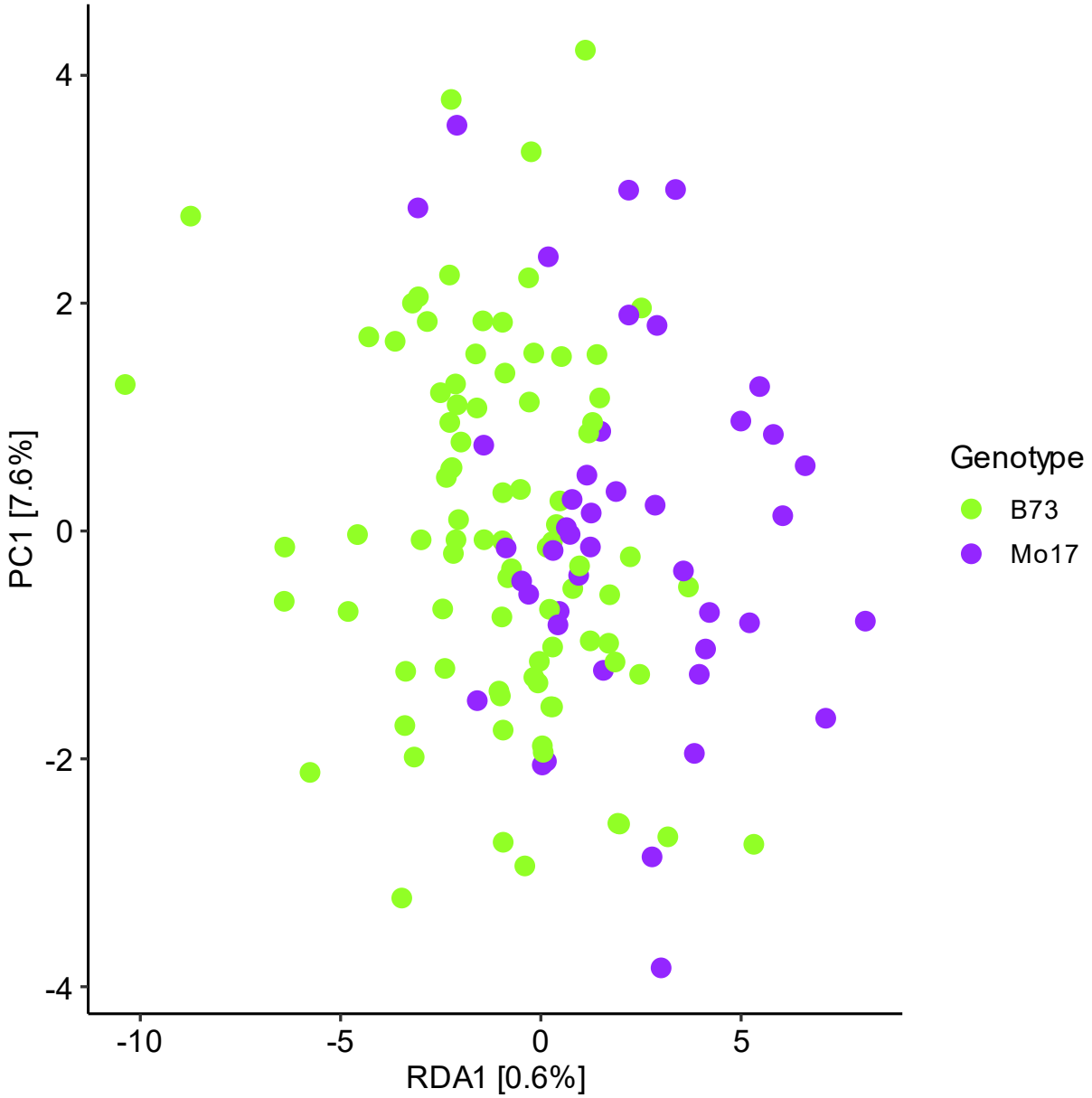

Figure S10. Redundancy analysis for fungal community composition. Points are colored by maize genotype.

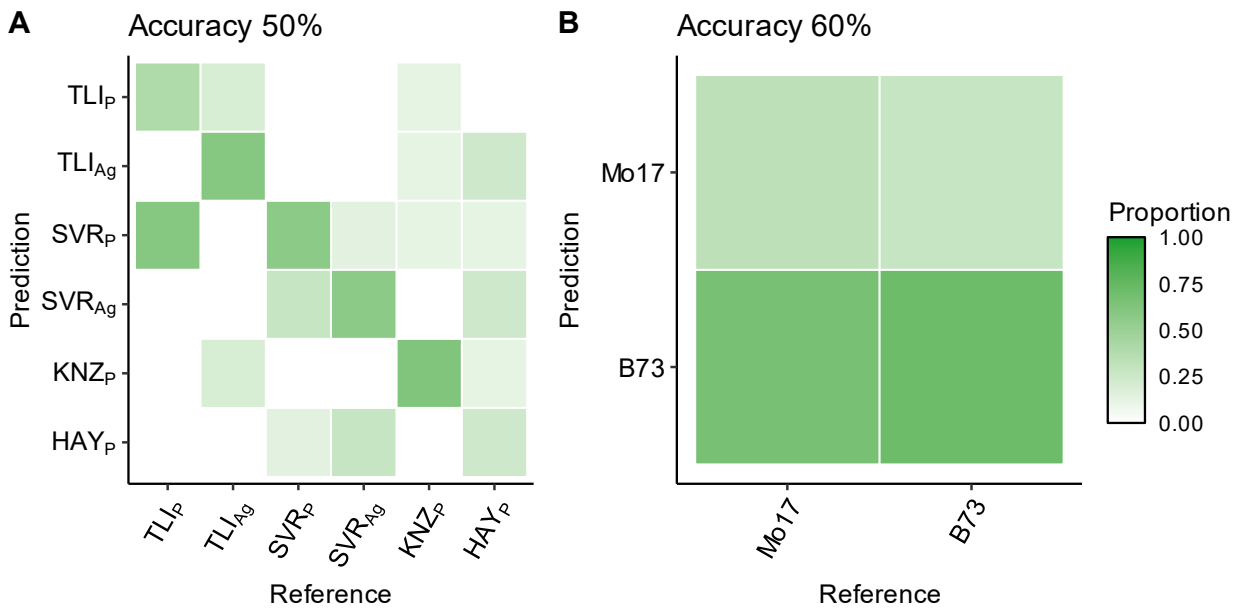

Figure S11. Confusion matrices depicting the classification accuracy of random forest classifiers trained on bacterial data predicting **A)** Soil Inoculum and **B)** Genotype. The models were trained using an 80:20 data split (80% train, 20% test) with 10-fold cross validation, shading represents the proportion of predictions for a label. Labels on the left represent the predicted labels and the labels on the bottom represent the actual labels. The model wide accuracy is given above each confusion matrix, class-wise statistics are provided in table in Table S8.

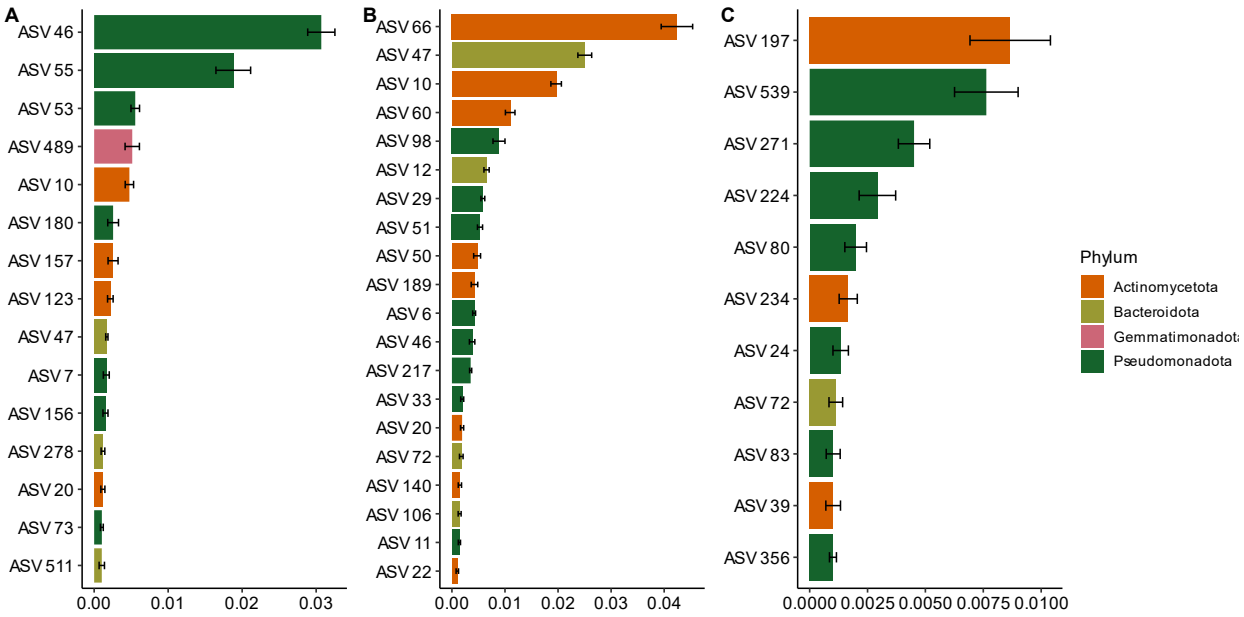

Figure S12. Bacterial ASV importance plots per random forest classifier. Results for **A)** Drought Treatment, **B)** Soil Inoculum, and **C)** Genotype classifiers. For each random forest classifier, 10-fold cross validation was used to assess the mean decrease in accuracy of the classifier when a particular ASV is withheld. Error bars represent the standard error across the 10-folds. Only ASVs with a mean decrease in accuracy greater than 0.001 are shown.

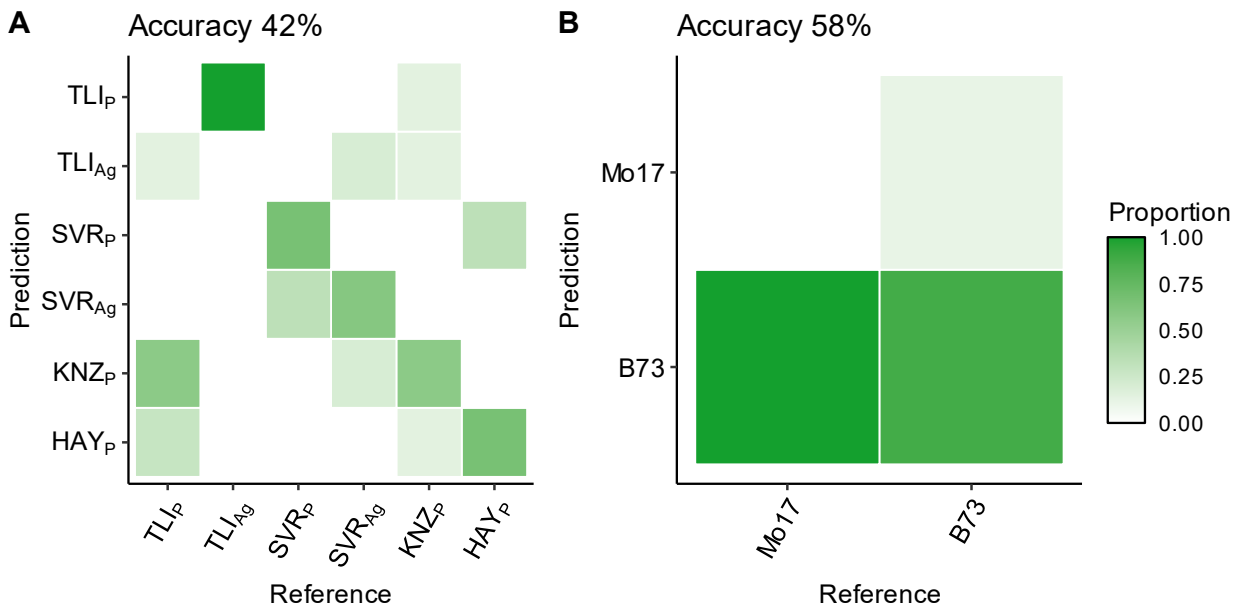

Figure S13. Confusion matrices depicting the classification accuracy of random forest classifiers trained on fungal data predicting **A)** Soil Inoculum and **B)** Genotype. The models were trained using an 80:20 data split (80% train, 20% test) with 10-fold cross validation, shading represents the proportion of predictions for a label. Labels on the left represent the predicted labels and the labels on the bottom represent the actual labels. The model wide accuracy is given above each confusion matrix, class-wise statistics are provided in table in Table S9.

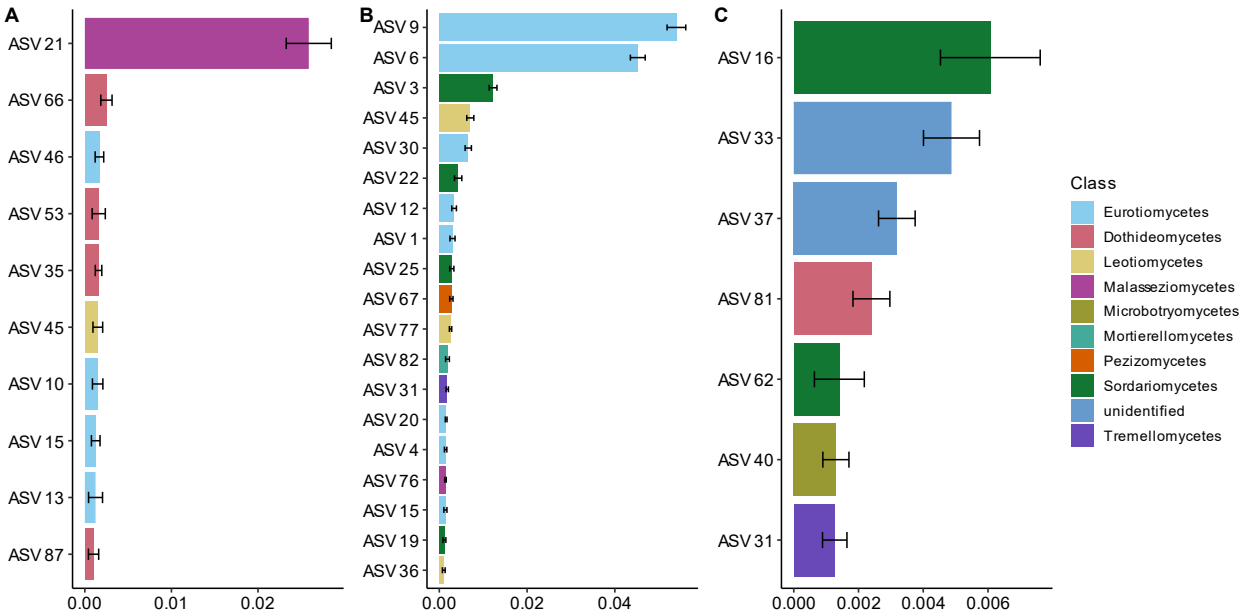

Figure S14. Fungal ASV importance plots per random forest classifier. Results for **A)** Drought Treatment, **B)** Soil Inoculum, and **C)** Genotype classifiers. For each random forest classifier, 10-fold cross validation was used to assess the mean decrease in accuracy of the classifier when a particular ASV is withheld. Error bars represent the standard error across the 10-folds. Only ASVs with a mean decrease in accuracy greater than 0.001 are shown.

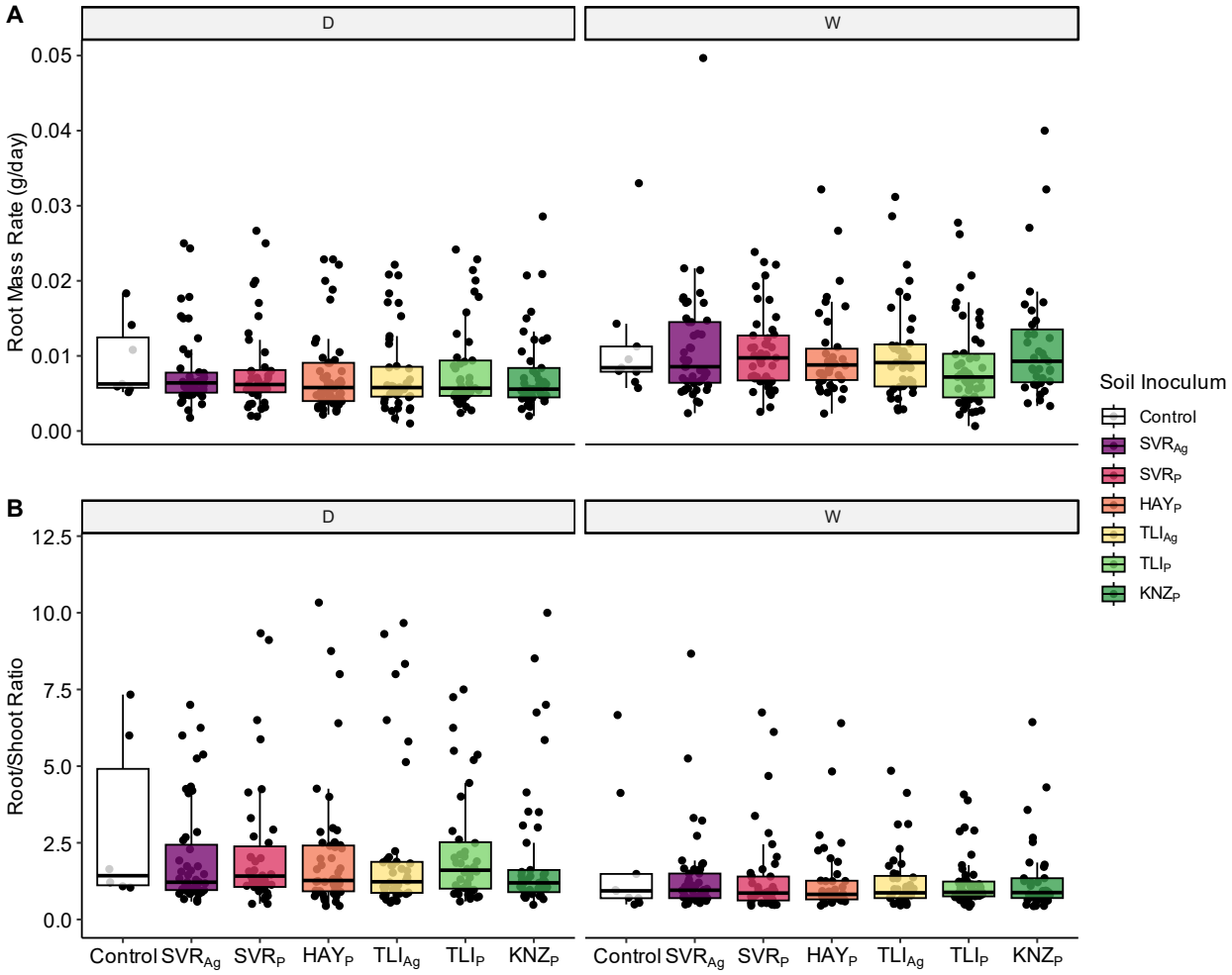

Figure S15. Root growth responses by soil inoculum. Boxplots are colored by soil inoculum for **A)** root mass rate and **B)** root/shoot ratio (four R/S data points were removed to reduce the y axis range and aid in visualization). Separate facets represent drought (D) and well-watered plants (W). Boxplot hinges represent the 1st and 3rd quartiles; whiskers represent 1.5 times the interquartile range.

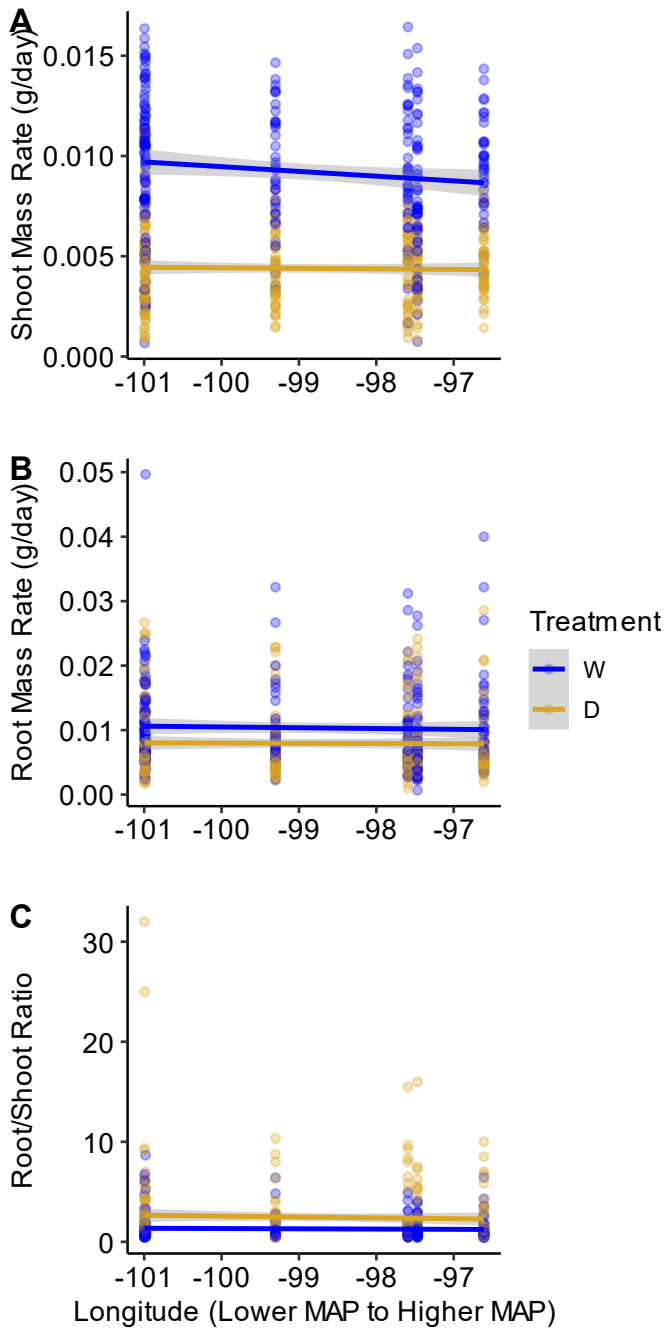

Figure S16. Plant growth responses across longitude for all soil inocula. For each growth response **A**) shoot mass rate, **B**) root mass rate, **C**) root/shoot ratio we plot the distribution and trend line for well-watered and droughted plants.

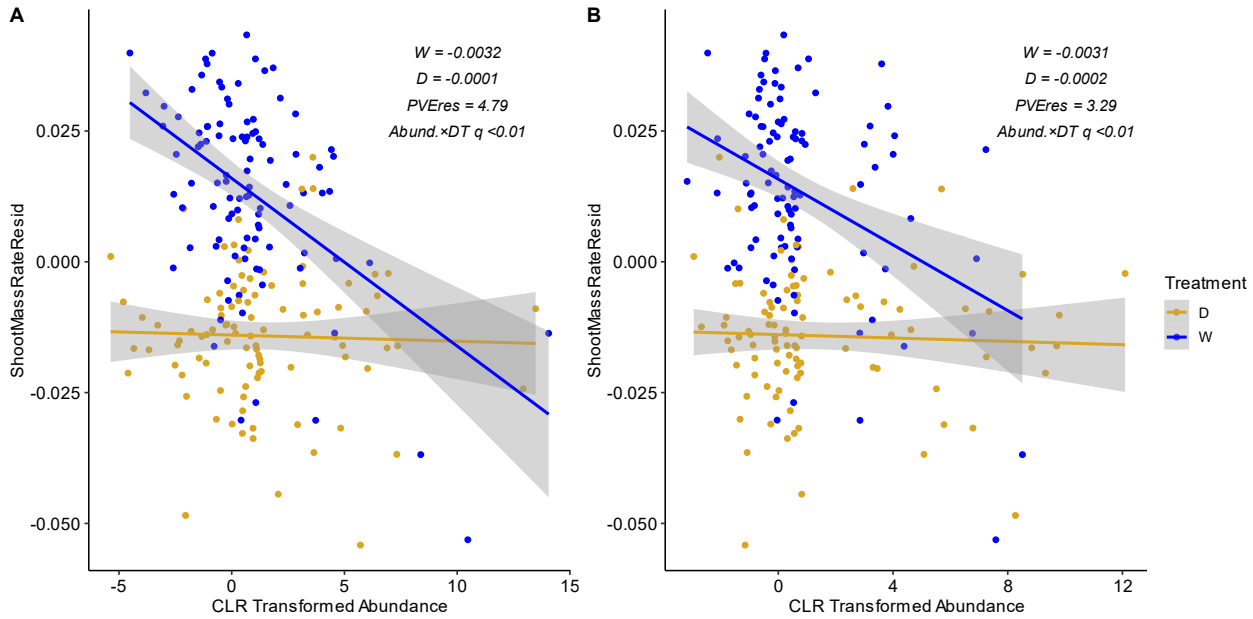

Figure S17. Bacterial families **A)** Corynebacteriaceae and **B)** Streptococcaceae show a significant interaction between CLR transformed abundance and drought treatment for shoot mass rate.

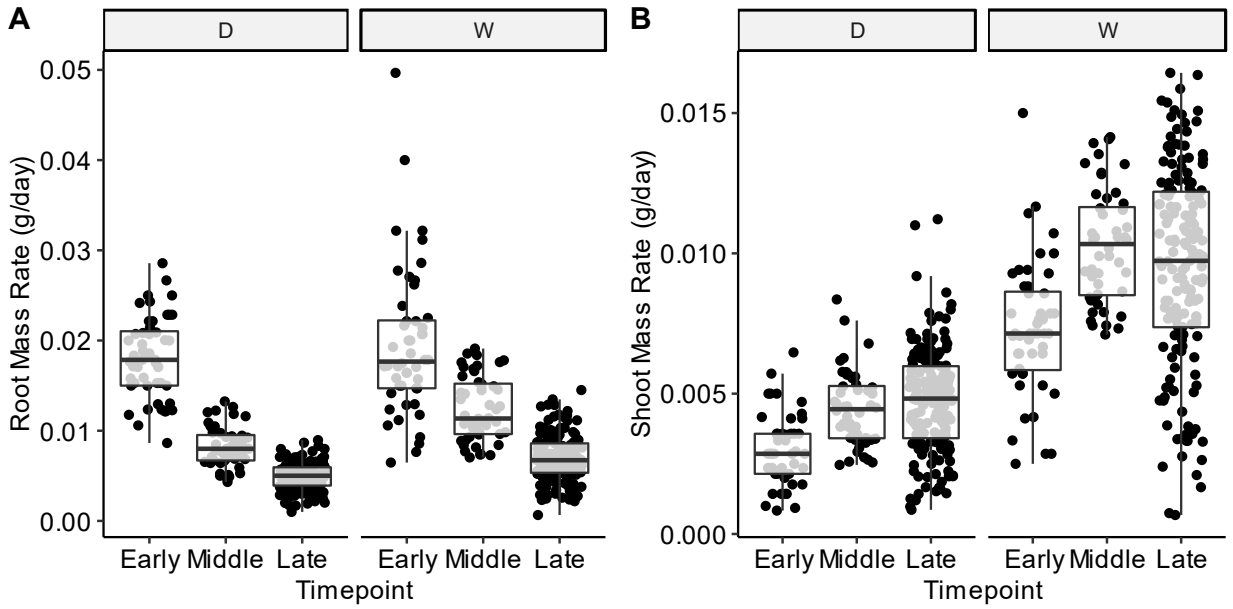

Figure S18. Plant growth rates across the collection time points of the study. A) Root mass rate tended to decrease over the course of the experiment and was modulated by the drought treatment (ANOVA; *'Timepoint × Treatment'* p-value< 0.01). **B**) Shoot mass rate tended to increase over the course of the experiment (ANOVA; *'Timepoint'* p-value< 0.01).

Supplemental Tables

Table S1. ANOVA table for maize emergence rate.

	DF	ChiSq	*p*-value
Intercept	1	1072.80	**<0.01**
Genotype (G)	1	7.28	**0.01**
Soil Inoculum (SI)	5	5.42	0.37
G x SI	5	5.97	0.31

Bold values denote significant effects, *p*-value<0.05

Table S2. ANOVA table for bacterial alpha diversity metrics of soil samples collected from six locations across the Kansas precipitation gradient.

		log(Chao1)			**log(Shannon's Diversity)**			**log(Inverse Simpson Diversity)**		
Factor	DF	SS	*F*-value	*p*-value	SS	*F*-value	*p*-value	SS	*F*-value	*p*-value
Substrate	1	0.57	1.14	0.29	0.08	0.11	0.74	0.01	0.01	0.92
Collection Site	5	15.9	6.37	**<0.01**	14.41	4.24	**<0.01**	10.67	3.29	**0.01**
Sequence Depth	1	81.02	162.34	**<0.01**	58.20	85.58	**<0.01**	36.96	57.06	**<0.01**
Residual	52	25.95			35.36			33.68		

Bold values denote significant effects, *p*-value<0.05

Table S3. ANOVA table for fungal alpha diversity metrics of soil samples collected from six locations across the Kansas precipitation gradient.

		log(Chao1)			**log(Shannon's Diversity)**			**log(Inverse Simpson Diversity)**		
Factor	DF	SS	*F*-value	*p*-value	SS	*F*-value	*p*-value	SS	*F*-value	*p*-value
Substrate	1	10.50	45.07	**<0.01**	0.02	0.08	0.78	2.99	7.16	**0.01**
Collection Site	5	3.07	2.64	**0.03**	2.67	1.75	0.13	5.21	2.5	**0.04**
Sequence Depth	1	14.67	62.99	**<0.01**	0.45	1.47	0.23	1.28	3.07	0.08
Residual	81	18.87			24.69			33.79		

Bold values denote significant effects, *p*-value<0.05

Table S4. PERMANOVA table for bacterial and fungal community composition of soil and inocula samples collected from six locations across the Kansas precipitation gradient.

	Bacteria					**Fungi**				
Factor	DF	SS	R^2	*F-value*	*p-value*	DF	SS	R^2	*F-value*	*p-value*
Substrate	1	44584	0.10	7.93	**<0.01**	1	32134	0.07	8.05	**<0.01**
Collection Site	5	101664	0.23	3.62	**<0.01**	5	101753	0.22	5.1	**<0.01**
Residual	53	297985	0.67			82	327269	0.71		

Bold values denote significant effects, *p*-value<0.05

Table S5. ANOVA table for bacterial alpha diversity metrics of maize nodal roots.

		Chao1			log(Shannon's Diversity)			log(Inverse Simpson Diversity)		
Factor	DF	SS	F-value	*p*-value	SS	*F*-value	*p*-value	SS	*F*-value	*p*-value
Genotype (G)	1	38929	2.23	0.14	0.17	0.39	0.53	0.02	0.06	0.80
Soil Inoculum (SI)	5	128720	1.48	0.2	4.11	1.92	0.09	3.46	1.81	0.11
Drought Treatment (DT)	1	110485	6.34	**0.01**	0.01	0.03	0.87	0.17	0.45	0.50
SI x DT	5	57853	0.66	0.65	2.35	1.10	0.36	2.72	1.43	0.22

Bold values denote significant effects, *p*-value<0.05

Table S6. ANOVA table for fungal alpha diversity metrics of maize nodal roots.

		Chao1			log(Shannon's Diversity)			log(Inverse Simpson Diversity)		
Factor	DF	SS	*F*-value	*p*-value	SS	*F*-value	*p*-value	SS	*F*-value	*p*-value
Genotype (G)	1	36.25	0.20	0.66	0.17	0.43	0.51	0.17	0.46	0.50
Soil Inoculum (SI)	5	1221.90	1.33	0.26	1.74	0.89	0.49	1.30	0.72	0.61
Drought Treatment (DT)	1	15.85	0.09	0.77	1.04	2.67	0.11	0.77	2.13	0.15
SI x DT	5	1496.80	1.63	0.16	5.95	3.06	**0.01**	5.21	2.89	**0.02**

Bold values denote significant effects, *p*-value<0.05

Table S7. Optimal hyperparameters for bacterial and fungal machine learning classifiers trained to predict treatment, soil inoculum, and genotype.

	Bacteria		Fungi	
Factor	mtry	Minimum Node Side	mtry	Minimum Node Side
Treatment	559	10	64	10
Soil Inoculum	437	5	46	5
Genotype	559	5	10	1

Table S8. Output statistics for bacterial machine learning models predicting treatment, genotype, and soil inoculum.

Metric	Treatment	Genotype	Soil Inoculum					
			SVR_P	SVR_{Ag}	HAY_P	TLI_P	TLI_{Ag}	KNZ_P
Precision	0.737	0.714	0.400	0.500	0.400	0.500	0.500	0.714
Recall	0.700	0.714	0.571	0.571	0.250	0.400	0.600	0.625
F1	0.718	0.714	0.471	0.533	0.308	0.444	0.546	0.667
Prevalence	0.500	0.700	0.175	0.175	0.200	0.125	0.125	0.200
Balanced Accuracy	0.725	0.524	0.695	0.725	0.578	0.671	0.757	0.781

Table S9. Output statistics for fungal machine learning models predicting treatment, genotype, and soil inoculum.

Metric			Soil Inoculum					
	Treatment	Genotype	SVR_P	SVR_{Ag}	HAY_P	TLI_P	TLI_{Ag}	KNZ_P
Precision	0.500	0.625	0.667	0.750	0.400	0.000	0.000	0.444
Recall	0.462	0.8824	0.667	0.600	0.667	0.000	0.000	0.571
F1	0.480	0.7317	0.667	0.667	0.500	NA	NA	0.500
Prevalence	0.500	0.6538	0.115	0.192	0.115	0.269	0.038	0.269
Balanced Accuracy	0.500	0.4412	0.812	0.776	0.768	0.447	0.440	0.654